Cell Reports

Article

Interspecies Comparative Analyses Reveal Distinct Carbohydrate-Responsive Systems among *Drosophila* Species

Graphical Abstract

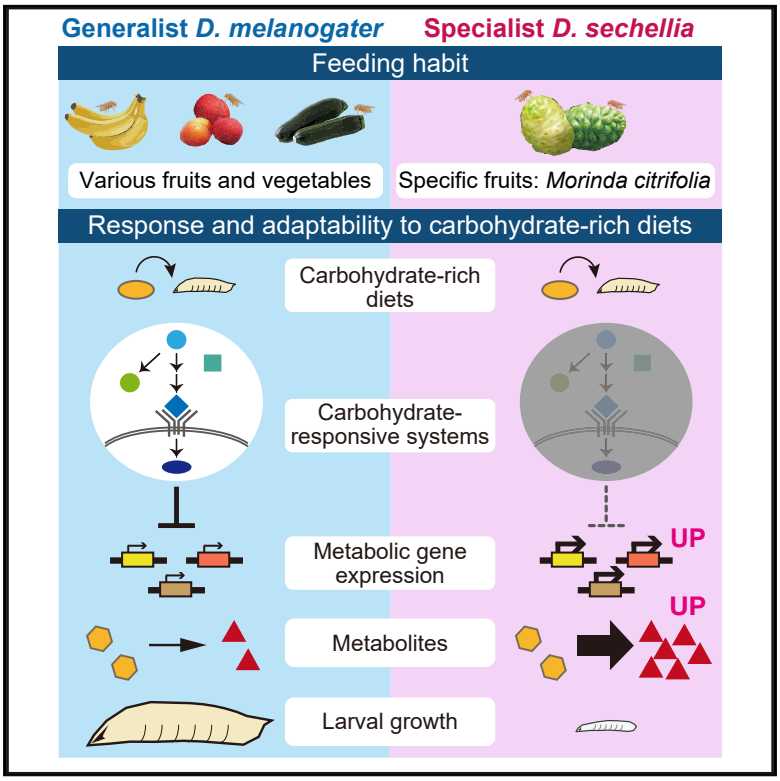

Authors

Kaori Watanabe, Yasutetsu Kanaoka, Shoko Mizutani, ..., Masayoshi Watada, Tadashi Uemura, Yukako Hattori

Correspondence

tauemura@lif.kyoto-u.ac.jp (T.U.), yhattori@lif.kyoto-u.ac.jp (Y.H.)

In Brief

Watanabe et al. uncover robust carbohydrate-responsive regulatory systems, including TGF-β/Activin signaling, which allow larvae of a generalist *Drosophila melanogaster* to adapt to various nutrient balances. In contrast, a specialist *D. sechellia* is defective in the systems and no longer maintains metabolic homeostasis, culminating in reduced adaptation to carbohydrate-rich diets.

Highlights

- The generalists adapt to various nutrient balances, whereas the specialists cannot
- The generalists regulate carbohydrate-responsive gene expression by Activin signaling
- The specialist species are defective in carbohydrate-responsive gene regulation
- The specialist *D. sechellia* accumulates various metabolites and reduces adaptation

Watanabe et al., 2019, Cell Reports *28*, 2594–2607
September 3, 2019
https://doi.org/10.1016/j.celrep.2019.08.030

CellPress

OPEN ACCESS
CellPress

Cell Reports
Article

Interspecies Comparative Analyses Reveal Distinct Carbohydrate-Responsive Systems among *Drosophila* Species

Kaori Watanabe,[1] Yasutetsu Kanaoka,[1] Shoko Mizutani,[1] Hironobu Uchiyama,[2] Shunsuke Yajima,[2,3] Masayoshi Watada,[4] Tadashi Uemura,[1,5,6,*] and Yukako Hattori[1,7,*]

[1]Graduate School of Biostudies, Kyoto University, Kyoto 606-8501, Japan
[2]NODAI Genome Research Center, Tokyo University of Agriculture, Tokyo 156-8502, Japan
[3]Department of Bioscience, Tokyo University of Agriculture, Tokyo 156-8502, Japan
[4]Graduate School of Science and Engineering, Ehime University, Matsuyama 790-8577, Japan
[5]Research Center for Dynamic Living Systems, Kyoto University, Kyoto 606-8501, Japan
[6]AMED-CREST, AMED, 1-7-1 Otemachi, Chiyoda-ku, Tokyo 100-0004, Japan
[7]Lead Contact
*Correspondence: tauemura@lif.kyoto-u.ac.jp (T.U.), yhattori@lif.kyoto-u.ac.jp (Y.H.)
https://doi.org/10.1016/j.celrep.2019.08.030

SUMMARY

During evolution, organisms have acquired variable feeding habits. Some species are nutritional generalists that adapt to various food resources, while others are specialists, feeding on specific resources. However, much remains to be discovered about how generalists adapt to diversified diets. We find that larvae of the generalists *Drosophila melanogaster* and *D. simulans* develop on three diets with different nutrient balances, whereas specialists *D. sechellia* and *D. elegans* cannot develop on carbohydrate-rich diets. The generalist *D. melanogaster* downregulates the expression of diverse metabolic genes systemically by transforming growth factor β (TGF-β)/Activin signaling, maintains metabolic homeostasis, and successfully adapts to the diets. In contrast, the specialist *D. sechellia* expresses those metabolic genes at higher levels and accumulates various metabolites on the carbohydrate-rich diet, culminating in reduced adaptation. Phenotypic similarities and differences strongly suggest that the robust carbohydrate-responsive regulatory systems are evolutionarily retained through genome-environment interactions in the generalists and contribute to their nutritional adaptabilities.

INTRODUCTION

Nutrition is a critical environmental determinant for animal growth, reproduction, and longevity. Through interactions with surrounding nutritional environments, animals have evolved their own feeding habits. Some species are generalists, which adapt to a wide range of food resources, while others are specialists, which feed on limited resources. Tight associations of specialists to their specific resources have been studied from the perspectives of food preference and toxin resistance (Johnson et al., 2018; Zhan et al., 2011). However, it is still unclear how adaptabilities to nutritional conditions differ between generalist and specialist species, how different responses are in gene regulation and metabolism, and what molecular mechanisms underlie the difference.

Drosophila melanogaster is an emerging model organism to study nutritional adaptability, which can be assessed by measuring the effects of diet on life history traits, such as developmental rate, fertility, and lifespan. Many inter-organ signaling molecules, such as *Drosophila* insulin-like peptides (Dilps), which have been functionally conserved during evolution, mediate nutrient responses (Droujinine and Perrimon, 2016). In nature, *Drosophila* species exhibit enormous variation in feeding habits. *D. melanogaster* and *D. simulans* are generalists that are globally distributed and able to breed on a wide variety of rotting fruits, vegetables, and other plant matter (Figure 1A) (Markow, 2015; Markow and O'Grady, 2008). In contrast, *D. sechellia*, *D. erecta*, and *D. elegans* are specialists that have limited habitats and reproduce on specific fruits or flowers (Figure 1A) (Chandler et al., 2011; Hirai and Kimura, 1997; Markow, 2015; Markow and O'Grady, 2008; Rio et al., 1983; Tsacas and Bächli, 1981). For example, *D. sechellia* only lives in the Seychelles islands, and it feeds on a single host plant, *Morinda citrifolia*. Biogeographical and phylogenetic evidence suggests that *D. sechellia* evolved in isolation after colonization of these islands by its sister species, a generalist *D. simulans* (Clark et al., 2007; Hey and Kliman, 1993; Kliman et al., 2000). Previous studies on *Drosophila* specialist species have provided examples of the genetic underpinnings of traits that are adaptive to their host resources, such as chemoreception and egg production (Lang et al., 2012; Lavista-Llanos et al., 2014; Linz et al., 2013; Matsuo et al., 2007; McBride et al., 2007). It was also reported that nutritional adaptability and gene expression are different between *D. melanogaster* and cactus-feeding species (Matzkin et al., 2011; Nazario-Yepiz et al., 2017); however, the underlying molecular mechanisms of these differences have not been resolved.

Here, we address the aforementioned questions by comparing adaptability (larval growth), nutritional profiles in natural food

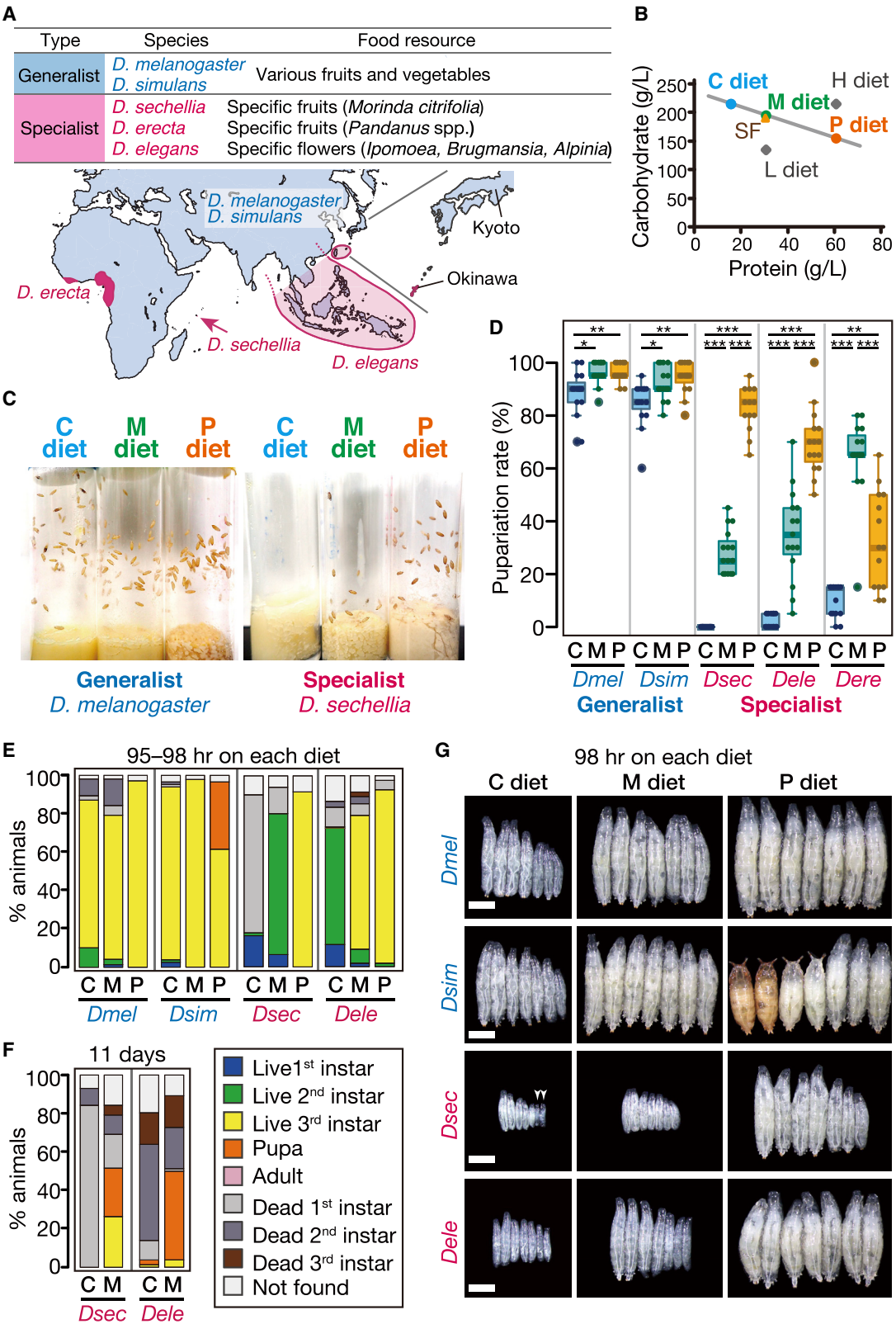

(legend on next page)

resources, and transcriptional and metabolic responses to diets among the five *Drosophila* species (Figure 1A). We first examined whether there is a difference in adaptability to a range of nutrient balances among the species. To define the nutrient balances, we focused on protein-to-carbohydrate (P:C) ratios, which have a profound impact on lifespan and reproduction in mammals and insects (Matzkin et al., 2011; Matavelli et al., 2015; Simpson et al., 2015). For example, the lifespan in *D. melanogaster* is longer on low P:C ratio diets (Lee et al., 2008), and longevity in mice is also greatest on low P:C ratio diets (Solon-Biet et al., 2014). Diets for *D. melanogaster* with different P:C ratios in previous studies were made by varying the ratio of yeast to sucrose; therefore, P:C ratios for *D. melanogaster* also reflect the balance between yeast-derived nutrients and sugar. We found that larvae of the generalists adapted to all three diets with different P:C ratios tested, whereas the specialists *D. sechellia* and *D. elegans* could not adapt to carbohydrate-rich diets. We compared nutritional profiles of natural food resources for the species and investigated the critical impediments to adaptation of the specialists *D. sechellia* and *D. elegans*. Collectively, these results suggest that the generalists have adapted to foods with widely varying carbohydrate contents, whereas the specialists *D. sechellia* and *D. elegans* have lost this adaptability.

In the generalist *D. melanogaster*, the consumption of nutritive sugars stimulates the expression and secretion of the Activin-like ligand Dawdle (Daw) from the fat body. Daw then activates transforming growth factor β (TGF-β)/Activin signaling in the gut and represses expression of carbohydrases in response to the nutritional state (Chng et al., 2014). In addition, loss of TGF-β/Activin signaling leads to accumulation of tricarboxylic acid (TCA) cycle intermediates and upregulation of TCA cycle enzyme genes (Ghosh and O'Connor, 2014). TGF-β/Activin signaling also regulates muscle proteostasis and aging (Bai et al., 2013; Langerak et al., 2018). We performed RNA sequencing (RNA-seq) analysis using larval whole bodies and multiple tissues and found that the generalist *D. melanogaster* systemically regulated the expression of diverse metabolic genes by TGF-β/Activin signaling, while the specialists *D. sechellia* and *D. elegans* expressed those metabolic genes at higher levels on the carbohydrate-rich diet. Moreover, metabolomic analysis showed that the wild-type generalist *D. melanogaster* maintained metabolic homeostasis, whereas the specialist *D. sechellia* accumulated various metabolites on the carbohydrate-rich diet, as did the *D. melanogaster daw* mutant. We discuss both phenotypic similarities and differences among the species and the *D. melanogaster* mutants and the possible genetic changes of the carbohydrate-responsive systems in the specialists.

RESULTS

The Generalists Adapt to Various Nutrient Balances, whereas the Specialists Cannot

We first examined whether there is a difference in adaptability to a range of nutrient balances among the five *Drosophila* species above. We examined larval growth of the species on three isocaloric diets with different P:C ratios (Figure 1B; Table S1A): high-carbohydrate diet (C diet), medium diet (M diet), and high-protein (high-yeast) diet (P diet). We found that the larvae of the two generalist species developed into pupae on all three diets (Figures 1C and 1D). In contrast, larvae of all three specialists failed to develop on the C diet; most notably, two specialists, *D. sechellia* and *D. elegans*, reduced their pupariation rates proportionately with decreasing P:C ratios (Figures 1C and 1D; as for *D. erecta*, see Discussion). Larvae of the specialists *D. sechellia* and *D. elegans* showed substantial developmental delays on the C and M diets compared to the P diet (Figures 1E, 1G, and S1A). Importantly, more than 80% of *D. sechellia* larvae died at the first-instar stage, and 50% of *D. elegans* died at the second-instar stage on the C diet (Figure 1F), indicating that the critical timings of lethality were the first-instar stage in *D. sechellia* and the second-instar stage in *D. elegans*.

We next quantified food intake and addressed the possibility that the specialists, in particular *D. sechellia*, have feeding defects on the C and M diets and fail to develop on the diets. We found that the amount of food ingested by *D. sechellia* was less than the amount ingested by *D. melanogaster* on all three diets (Figures S1B and S1C), suggestive of species differences (see STAR Methods, "Designs for interspecies and omics analyses"). We therefore compared phenotypes among the three diets within each species rather than between the species on the same diet. *D. sechellia* as well as *D. melanogaster* did ingest a comparable amount of each food, regardless of the P:C ratio (Figures S1B and S1C). This result suggests that the poor adaptability of *D. sechellia* to the C and M diets compared to the P diet was not due to lower amounts of food intake on the diets. We also examined whether the associated microbes of the species played integral roles in their distinct adaptations by swapping their associated microbes. The specialist *D. sechellia*

Figure 1. The Generalists Adapt to Various Nutrient Balances, whereas the Specialists Cannot

(A) Generalist and specialist *Drosophila* species employed in this study and their natural food resources. *D. melanogaster* and *D. simulans* are cosmopolitan, globally distributed species, whereas the three specialists have limited habitats (highlighted in magenta).

(B) Contents of protein and carbohydrate in our experimental diets. The gray line represents isocaloric diets. SF: our laboratory standard food.

(C) Images of the generalist *D. melanogaster* (left) and specialist *D. sechellia* (right) fed on the individual diets. 60 first-instar larvae were placed on the diet in each vial. In this figure, "*D. melanogaster*" represents the wild-type *D. melanogaster Canton-Special* (*CS*) strain.

(D) Pupariation rates of 5 species. Each point indicates the percentage of pupated animals out of 20 first-instar larvae in a 1.5 mL tube with each respective diet. The central lines indicate the median. Boxes show the 25th–75th percentiles. Whiskers extend to the most extreme data points, which are no more than 1.5 times the interquartile range. *Dmel*, *D. melanogaster*; *Dsim*, *D. simulans*; *Dsec*, *D. sechellia*; *Dele*, *D. elegans*; *Dere*, *D. erecta*. *$p < 0.05$, **$p < 0.01$, and ***$p < 0.001$ (Steel-Dwass test, n = 13–15).

(E) Developmental stages of *D. melanogaster*, *D. simulans*, *D. sechellia*, and *D. elegans* at 95–98 h after first-instar larvae were placed on each diet (n = 80–100).

(F) Developmental stages of *D. sechellia* and *D. elegans* at 11 days after first-instar larvae were placed on the C or M diet (n = 80).

(G) Representative images of animals at 98 hours after first-instar larvae were placed on the individual diets. Arrowheads indicate dead larvae. Scale bars, 1 mm. See also Figure S1 and Table S1.

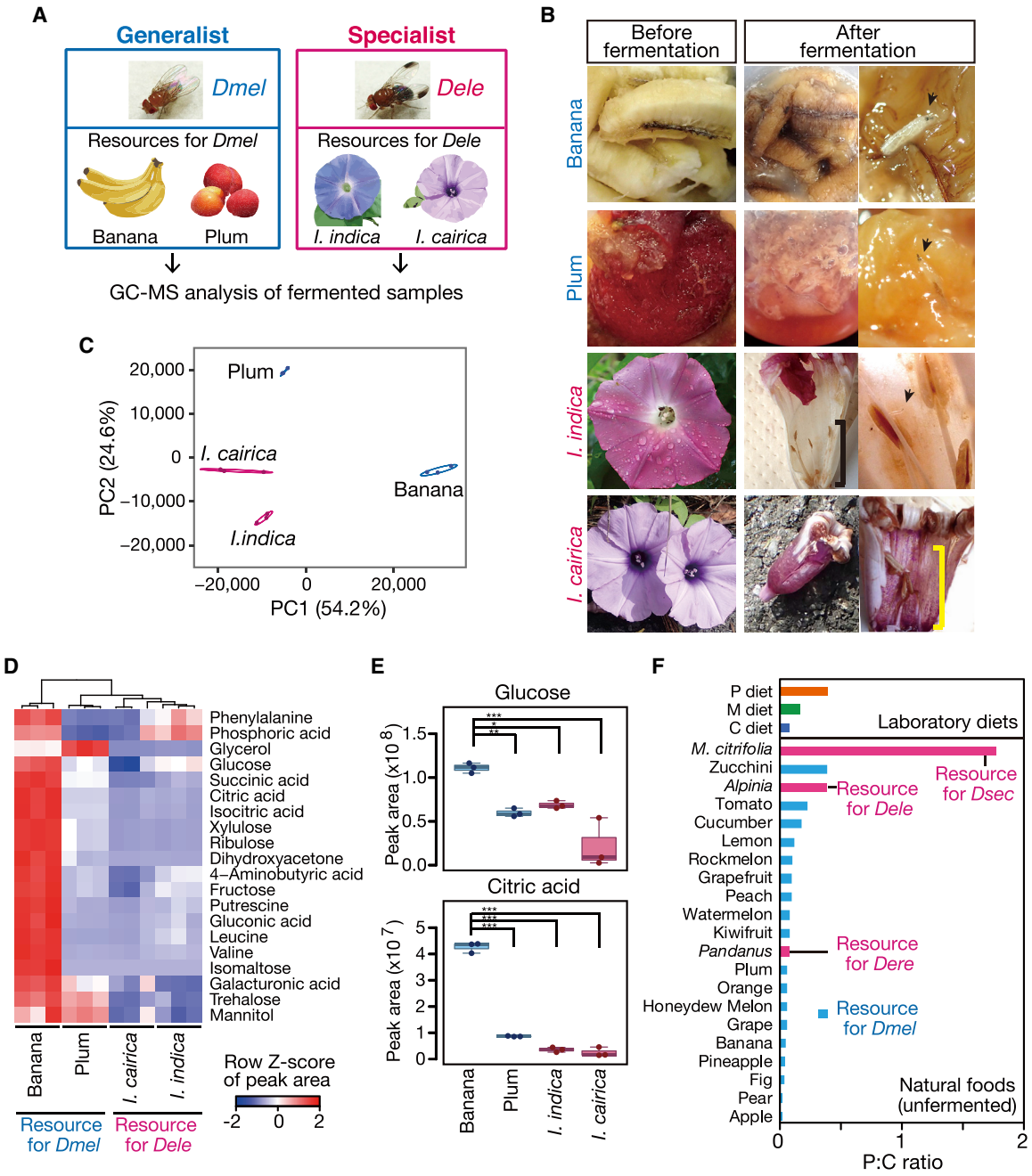

Figure 2. The Generalists Adapt to Much Higher Dietary Carbohydrates Than the Specialists, Both in the Wild and the Laboratory

(A) Experimental design for GC-MS analysis of fermented natural food resources for the generalist *D. melanogaster* (banana and plum) or the specialist *D. elegans* (*I. indica* and *I. cairica*).

(B) Images of natural food resources for generalists or the specialist *D. elegans* before and after fermentation. All fermented foods were actually fed on by growing larvae of the individual species (shown by arrows). For two species of morning glory, we dissected flowers and collected fermented stamens, pistils, and pollen (shown by brackets).

(C) Principal component analysis of detected compounds in the fermented natural food resources showing that the individual resources were separated into distinct clusters (n = 3). The first principal component (PC1) accounts for 54.2% of the variance.

(D) A heatmap showing peak areas of the top 20 compounds with the largest contribution to PC1 in (C).

(E) Peak areas of glucose (top) and citric acid (bottom), which made large contributions to PC1 in (C). Boxplots are depicted as in Figure 1D. Dunnett's test was performed to compare the individual compound levels in banana with those in the other samples (*$p < 0.05$, **$p < 0.01$, and ***$p < 0.001$, n = 3).

(legend continued on next page)

transplanted with the generalist *D. melanogaster* microbes still showed a reduced pupariation rate on the M and the C diet (Figures S1D and S1E), indicating that mechanisms encoded in the generalists' genomes, rather than their associated microbes, critically contribute to their adaptations. Collectively, these results indicate that the generalists showed remarkable adaptability to nutrient balances, which included P:C ratios on which the specialists could not readily grow.

The Generalists Adapt to Much Higher Dietary Carbohydrates Than the Specialists, Both in the Wild and the Laboratory

To investigate the critical impediments for adaptations of the specialists, we examined and compared nutritional profiles of their natural food resources. In nature, *Drosophila* species feed on fruits or flowers fermented by yeasts and bacteria. These microbes, especially yeasts, are important nutrient sources for *Drosophila* species, providing many nutrients such as amino acids, sterols, B vitamins, and fatty acids that are not abundantly present in plant materials (Broderick and Lemaitre, 2012; Yamada et al., 2015). For example, the nutritional components in fresh banana alone cannot support the growth of germ-free *D. melanogaster* larvae unless the banana is inoculated with yeasts (Anagnostou et al., 2010). We therefore collected and analyzed fermented resources on which larvae in the wild had actually fed and developed to the second- or third-instar stage, with the aim of matching the degree of fermentation between the foods: fermented bananas or plums in fly trap bottles in Kyoto for generalists (Figures 1A, 2A, and 2B; Table S1B) and two species of fermented wild morning glory in Okinawa (*Ipomoea indica* and *Ipomoea cairica*) for the specialist *D. elegans* (Figures 1A, 2A, and 2B). As for wild morning glory, we dissected fermented flowers and collected stamens, pistils, and pollen, which are the parts that are typically fed on by *D. elegans* larvae (Figure 2B). Calculating the P:C ratios of fermented wild morning glory is difficult to perform because measuring total protein and carbohydrate levels by the standard nutrition analysis requires a large quantity (100–500 g) of each food (Greenfield and Southgate, 2003). Alternatively, we performed gas chromatography-mass spectrometry (GC-MS) analysis, which requires much less sample material (approximately 100 mg; see also STAR Methods). Principal component analysis of a total of 102 detected compounds showed that the individual food resources were separated into distinct clusters and that the first principal component (PC1) accounted for 54.2% of the variance (Figure 2C). We found that contents of sugars and organic acids in sugar metabolic pathways mainly contribute to PC1 and that a resource of the generalists, fermenting banana, contained much higher sugars and organic acids than not only the specialist's resource, two species of wild morning glory, but also another resource of the generalists, fermenting plum (Figures 2D and 2E; Tables S1C–S1E). This result shows that the generalists can adapt to both high-carbohydrate banana and low-carbohydrate plum, whereas the specialist *D. elegans* adapts only to low-carbohydrate morning glory.

As mentioned above, it is desirable to analyze and compare nutritional profiles of fermented natural food resources fed on by the larvae of each species. However, fermented food resources, especially those for *D. sechellia* and *D. erecta*, are difficult to collect because of their restricted habitats (Figure 1A). As an alternative, we obtained nutrition data of unfermented natural food resources for *D. melanogaster* (fruits and vegetables; Broderick and Lemaitre, 2012; Gibson et al., 1981), *D. sechellia* (*M. citrifolia* fruits), and *D. erecta* (*Pandanus* fruits) from public nutrition databases and nutrition data of a food resource for *D. elegans* (*Alpinia* flowers) from a previous study (Rachkeeree et al., 2018). We found that *D. melanogaster* feeds on both high-carbohydrate diets (e.g., apple, pear, and fig) and low-carbohydrate diets (e.g., zucchini, tomato, and cucumber) in the wild (Figures 2F and S2A–S2C). On the other hand, the food resources for *D. sechellia* and *D. elegans* showed higher P:C ratios (low-carbohydrate) than most of those for *D. melanogaster* (Figures 2F and S2A–S2C). Previous studies showed that, on Mauritius, various *Drosophila* generalist species were observed emerging from rotten *M. citrifolia* fruits, of which the toxic products were detoxified by microbes (David et al., 1989; R'Kha et al., 1991), indicating that generalist species also have adaptabilities to high P:C ratio diets, such as *M. citrifolia.* All these results strongly suggest that the generalists have adapted to foods with widely varying P:C ratios and can adapt to much higher dietary carbohydrates than the specialists *D. elegans* and *D. sechellia* in the wild. In addition, we compared P:C ratios of these natural food resources with those of laboratory diets (the C, M, and P diets). It should be noted that laboratory diets contain dry yeast as an alternative to microbes fermenting food resources in the wild, and P:C ratios of laboratory diets tend to be higher than those of unfermented natural food resources (Figure 2F). Therefore, a simple comparison is not sufficiently accurate; notwithstanding, the P:C ratio of the P diet was comparable to that of a natural food resource for *D. elegans* (Figure 2F), which was consistent with its highest adaptability to the P diet among the three laboratory diets.

The *D. melanogaster daw* Mutant Cannot Adapt to Carbohydrate-Rich Diets, Much Like the Specialists *D. sechellia* and *D. elegans*

In the generalist *D. melanogaster*, systemic TGF-β/Activin signaling functions as a carbohydrate-responsive mechanism (Chng et al., 2014; Ghosh and O'Connor, 2014). We therefore asked whether *D. melanogaster* mutants of a TGF-β/Activin ligand gene, *daw*, and its upstream regulator gene, *mlx* (Mattila et al., 2015), could adapt to our diets. The *daw* mutant larvae showed dramatically reduced pupariation rates on the M and the C diets (Figure 3A), closely resembling the specialists *D. sechellia* and *D. elegans* (Figure 1D). On the other hand, the *mlx* mutant larvae failed to adapt to not only the C diet, but

(F) Protein-to-carbohydrate ratios (P:C ratios) of our laboratory diets (the C, M, and P diets) and unfermented natural foods preferred by *D. melanogaster* (fruits and vegetables; described in Broderick and Lemaitre, 2012, and Gibson et al., 1981), *D. sechellia* (*M. citrifolia* fruits), *D. elegans* (*Alpinia* flowers), and *D. erecta* (*Pandanus* fruits). The data for the respective natural foods were sorted by their P:C ratios.
See also Figure S2, Table S1, and STAR Methods.

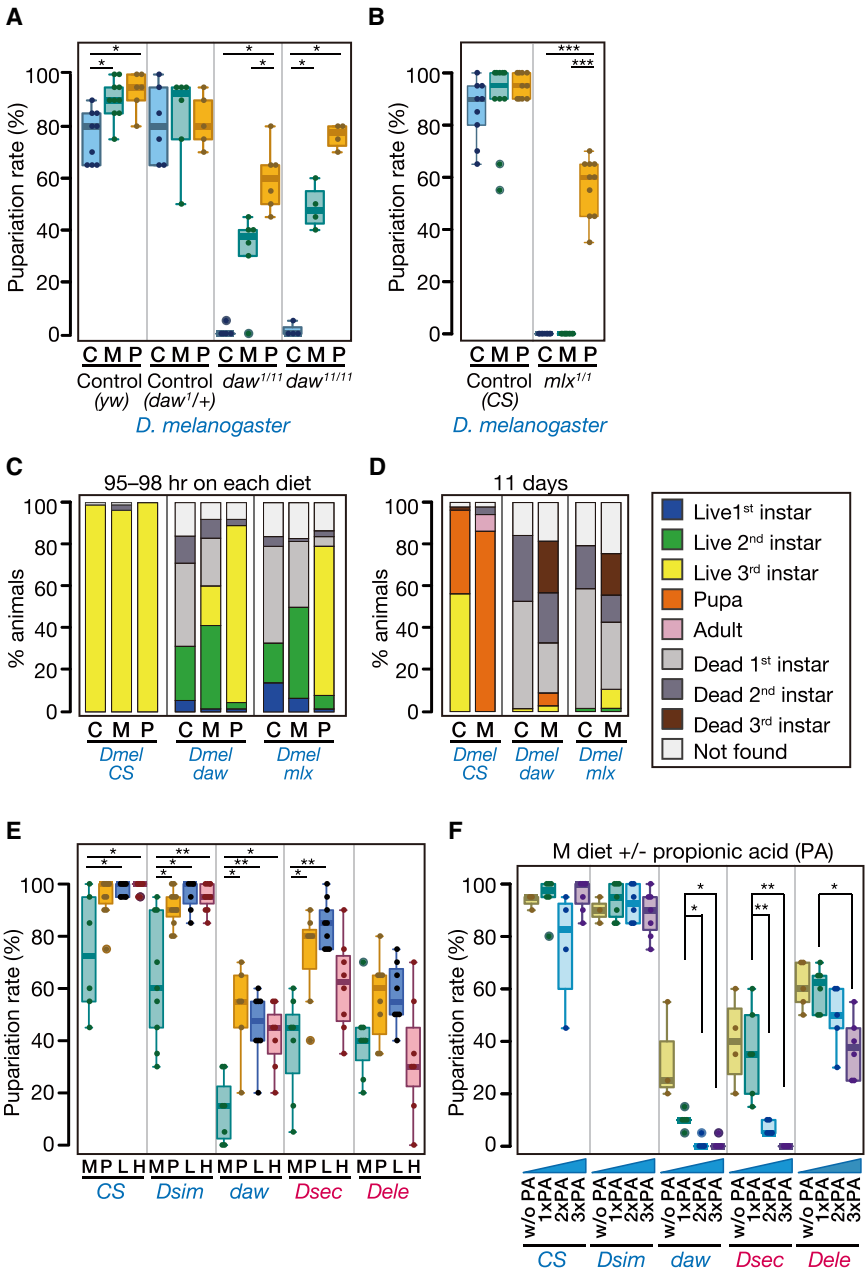

Figure 3. The *D. melanogaster daw* Mutant Cannot Adapt to Carbohydrate-Rich Diets, Much Like the Specialists *D. sechellia* and *D. elegans*

(A) Pupariation rates of control (*y w* and daw^{1}/+) and *daw* mutant ($daw^{1/11}$ and $daw^{11/11}$) *D. melanogaster* larvae on each diet in a 1.5 mL tube. (Steel-Dwass test, n = 4–10).

(B) Pupariation rates of control (*CS*) and *mlx* mutant ($mlx^{1/1}$) *D. melanogaster* larvae on each diet (Steel-Dwass test, n = 9–10).

(C) Developmental stages of the *D. melanogaster CS*, *daw* mutant ($daw^{1/11}$), and *mlx* mutant ($mlx^{1/1}$) at 95–98 h after first-instar larvae were placed on each diet (n = 80–100).

(D) Developmental stages of the *D. melanogaster CS*, *daw* mutant, and *mlx* mutant at 11 days after first-instar larvae were placed on the C or M diet (n = 80).

(E) Pupariation rates of the individual species or genotypes on the M diet, the P diet, the L diet, and the H diet (Steel test, n = 6–12). The L diet contains the same amount of sucrose as the P diet and the same amount of yeast as the M diet, whereas the H diet contains the same amount of sucrose as the M diet and the same amount of yeast as the P diet. See also Figure 1B and Table S1A.

(F) Pupariation rates of the individual species or genotypes on M diets with different amounts of propionic acid (PA; Steel test, n = 3–7). w/o PA, M diet without PA; 1xPA, M diet; 2xPA, M diet with 2x PA; 3xPA, M diet with 3x PA.

Boxplots in (A), (B), (E), and (F) are depicted as in Figure 1D. *p < 0.05, **p < 0.01, and ***p < 0.001.

also the M diet (Figure 3B), which is a more severe phenotype than those of the two specialists and the *daw* mutant. Next, we examined lethal stages of the *daw* and *mlx* mutants on our diets. We found that more than 50% of the *daw* mutant or *mlx* mutant larvae died at the first-instar stage on the C diet (Figures 3C and 3D). This result suggests that the critical timing of lethality was the first-instar stage in both the *daw* and *mlx* mutants, which resembles the timing of lethality of the specialist *D. sechellia* (Figures 1E and 1F). From these results, we mainly focused on phenotypic similarities between the specialist *D. sechellia* and the *D. melanogaster daw* mutant.

In addition to the three laboratory diets, we examined adaptabilities to a low-protein and low-carbohydrate diet and a high-protein and high-carbohydrate diet (L diet and H diet, respectively) (Figure 1B; Table S1A). Both the *daw* mutants and the specialists *D. sechellia* and *D. elegans* developed better on the L diet than the M diet (Figure 3E). This result suggests that their inability to adapt to the M or the C diet was due to the excess amounts of carbohydrates rather than the low-abundances of other yeast-derived nutrients. Intriguingly, pupariation rates of the *daw* mutant and the specialist *D. sechellia* tended to be higher on the H diet compared to the M diet (Figure 3E), indicating that the key variable to their adaptation is the ratio of carbohydrates to other yeast-derived nutrients in the foods rather than the total amount of carbohydrates. It was previously reported that the *daw* mutation reduced pupariation rates on propionic acid (PA; a mold inhibitor)-induced acidic diets (Ghosh and O'Connor, 2014). The specialists *D. sechellia* and *D. elegans* also showed reduced pupariation rates on the M diet with supplemental PA (Figure 3F). These observations raised the possibility that the specialists are defective in TGF-β/Activin signaling and unable to adapt to carbohydrate-rich and/or acidic diets.

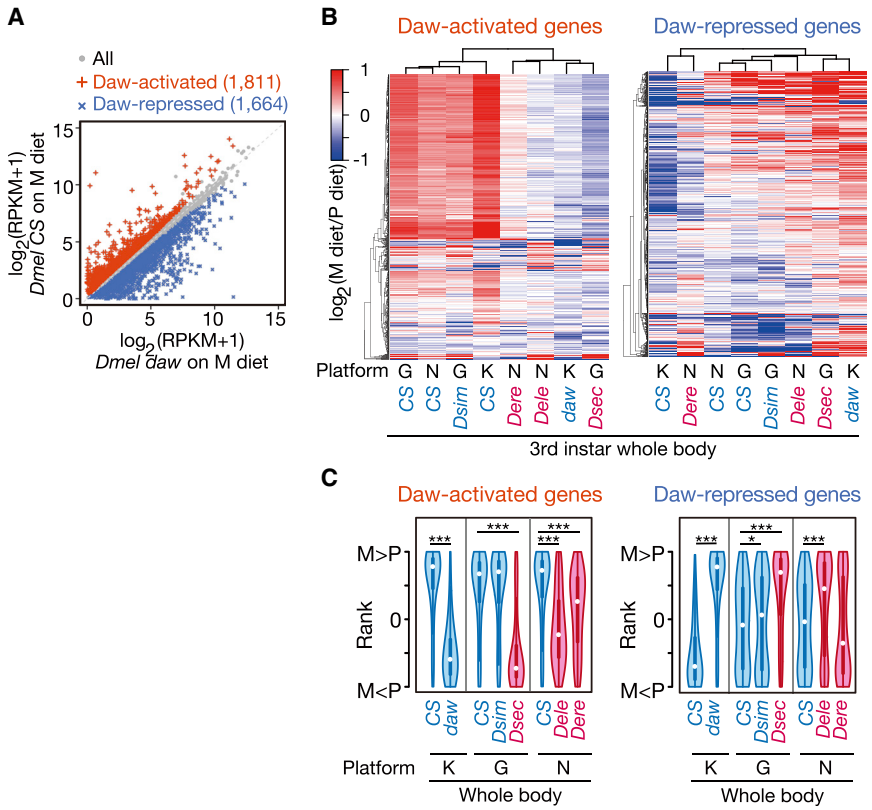

Figure 4. The Specialist Species Are Defective in Carbohydrate-Responsive Gene Regulation

(A) Scatterplot showing expression values in whole-body RNA-seq datasets of the wild-type *D. melanogaster CS* and the *daw* mutant at the wandering third-instar stage on the M diet.

(B) Heatmaps of whole-body expression profiles for the Daw-activated or Daw-repressed genes on the M diet at the wandering third-instar stage. RNA-seq platforms: K, Kyoto University; G, Genome Science; N, NODAI.

(C) Violin plots showing distributions of expression change between the diets for the Daw-activated or Daw-repressed genes by ranking. *$p < 0.05$ and ***$p < 0.001$ (Steel test or two-tailed Mann-Whitney *U* test, compared to the *D. melanogaster CS* on each platform). White circles indicate the median. Boxes show the 25th–75th percentiles. Whiskers extend to the most extreme data points, which are no more than 1.5 times the interquartile range. The shape denotes the density estimate and extends to extreme values.

See also Figures S3 and S4, Tables S2 and S6, and STAR Methods.

The Specialist Species are Defective in Carbohydrate-Responsive Gene Regulation and Express Metabolic Genes at Higher Levels on the Carbohydrate-Rich Diet

To examine whether carbohydrate-responsive gene regulation mediated by TGF-β/Activin signaling also functions in the specialists *D. sechellia* and *D. elegans*, we performed RNA-seq of larval whole bodies. To exclude the possibility that differences in developmental stage and sex influence the outcome of the experiments and lead to erroneous conclusions (Markow and O'Grady, 2005), we decided to use male larvae at the wandering third-instar stage that fed on the M or the P diet (see details in "Designs for interspecies and omics analyses" in STAR Methods). On the M diet, 1,811 genes were expressed at significantly higher levels in the wild-type *D. melanogaster Canton-Special* (*CS*) strain than the *daw* mutant, and we designated those as "Daw-activated genes" (red in Figure 4A and Table S2). In contrast, 1,664 genes showed lower expression levels on the M diet ("Daw-repressed genes"; blue in Figure 4A and Table S2). We then focused on these Daw-activated or Daw-repressed genes on the M diet and compared dietary responses (expression changes between the M and the P diet) among the five species and the *D. melanogaster daw* mutant by clustering or ranking (Figures 4B and 4C; Table S2). We found that the responses of the specialist *D. sechellia* and *D. elegans* were much closer to those of the *daw* mutants than the wild-type generalists (Figures 4B and 4C). Similar to the *daw* mutants, the two specialists expressed the Daw-activated genes at lower levels on the M diet and expressed the Daw-repressed genes at higher levels (Figures 4B and 4C), indicative of defective gene regulation of the Daw-activated and Daw-repressed genes.

We then addressed how gene regulation by TGF-β/Activin signaling operates in the adaptation of the generalists. Tissue-type-specific RNA-seq datasets (Brown et al., 2014) showed that Daw-activated genes are highly expressed mainly in the testis (Figure S3A). We addressed whether germline-less *D. melanogaster* male larvae, in which two Daw-activated genes that we tested were hardly expressed (Figures S3B and S3C), still adapted to the M and the C diets or not. Germline-less *D. melanogaster* still adapted to the M and the C diets, indicating that the testis-specific Daw-activated genes do not contribute appreciably to the adaptation (Figures S3B–S3D). In contrast, Daw-repressed genes show ubiquitous expression (Figure S4A). To search for tissues where TGF-β/Activin signaling plays an essential role in the nutritional adaptation, we knocked down a type I receptor gene of the signaling pathway *baboon* (*babo*) in a tissue-specific manner in *D. melanogaster.* We found that knocking down *babo* in muscles severely reduced pupariation rates on the C diet, suggesting that TGF-β/Activin signaling in muscles contributes to the adaptation (Figure S5A; see details in the legend). We therefore performed RNA-seq on muscles from wandering male larvae (Table S3). Of note, Daw-repressed genes in both whole bodies and muscles on the M diet were significantly enriched for enzyme-coding genes in diverse metabolic pathways (Figures 5A, S4B, S4C, S5B, and S5C; Tables S2 and S3). We then addressed whether the specialist *D. sechellia* can regulate the expression of these metabolic genes or not. Expression values for the metabolic Daw-repressed genes, not only in larval muscles, but also in guts and fat bodies of *D. sechellia*, were remarkably higher than

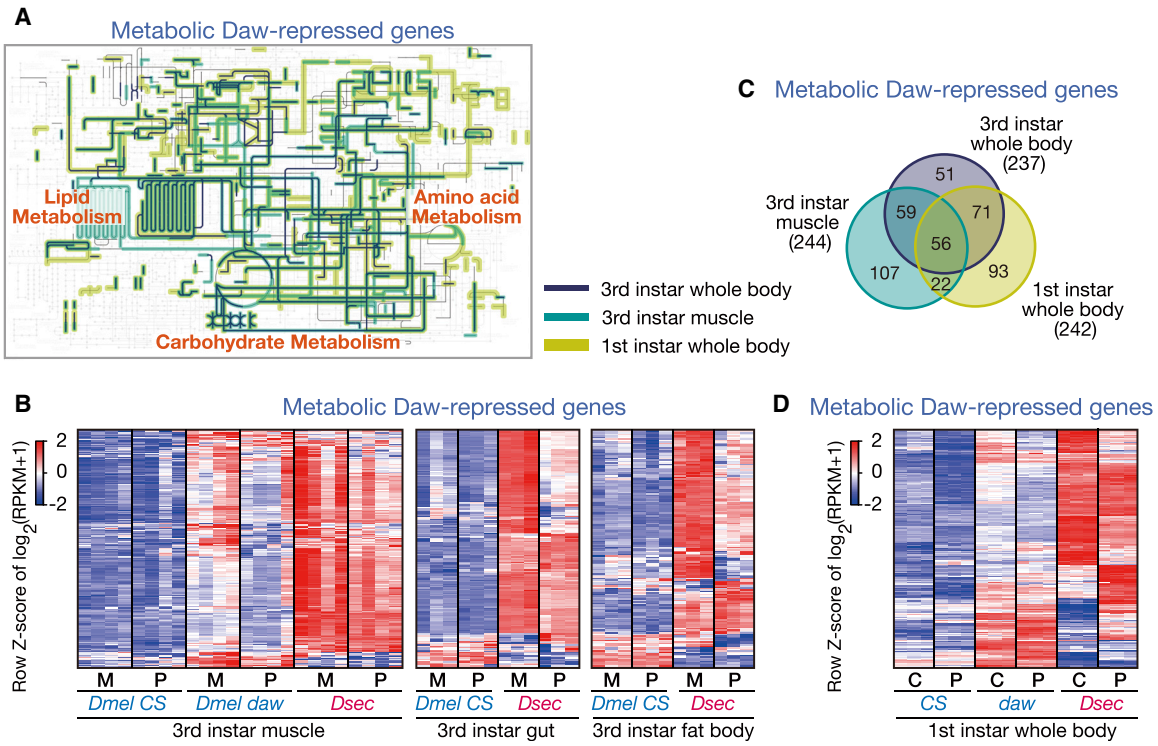

Figure 5. The Specialist *D. sechellia* Expresses Metabolic Genes at Higher Levels on the Carbohydrate-Rich Diet

(A) Metabolic pathways catalyzed by the Daw-repressed gene products in whole bodies and muscles of wandering third-instar larvae on the M diet and those in whole bodies of first-instar larvae on the C diet. Black lines indicate *D. melanogaster* metabolic pathways.

(B) Heatmaps of expression values for the metabolic Daw-repressed genes in muscles, guts, or fat bodies of the wild-type and the *daw* mutant *D. melanogaster* and *D. sechellia* at the wandering third-instar stage on the M or P diet.

(C) Venn diagrams showing overlaps among the metabolic Daw-repressed genes on the M diet in whole bodies, those in muscles of wandering third-instar larvae, and those on the C diet in whole bodies of first-instar larvae. The numbers of genes in the individual categories are indicated.

(D) A heatmap of expression values for the metabolic Daw-repressed genes in the wild-type and the *daw* mutant *D. melanogaster* and *D. sechellia* at the first-instar stage on the C or P diet.

See also Figures S4 and S5 and Tables S2, S3, S4, S5, and S6.

those of the wild-type *D. melanogaster*, in particular on the M diet (Figure 5B; Tables S3, S4, and S6).

We further examined whether these defects in gene regulation in wandering male larvae of the specialist *D. sechellia* on the M diet were also seen in larvae on the C diet, where most *D. sechellia* larvae eventually died at the first-instar stage (Figure 1F). For this purpose, we performed RNA-seq using first-instar larvae on the C or the P diet. On the C diet, 2,515 genes were expressed at significantly lower levels in the wild-type *D. melanogaster* than the *daw* mutant, and we designated those as "Daw-repressed genes on the C diet" (Table S5). These Daw-repressed genes include 242 metabolic genes; notably, they overlapped substantially with Daw-repressed genes of the third-instar-larval whole body or muscle on the M diet (Figures 5A, 5C, and S4D; Tables S5 and S6). In addition, many of the expression values of the metabolic Daw-repressed genes of the first-instar larvae were markedly higher in the specialist *D. sechellia* on the C diet—not only compared to the wild-type *D. melanogaster*, but also the *daw* mutant on the C diet (Figure 5D; Tables S5 and S6). All of these results indicate that the generalists can systemically downregulate metabolic gene expression levels by TGF-β/Activin signaling on the carbohydrate-rich M or C diet at both early and late larval stages, whereas the specialists *D. sechellia* and *D. elegans* show increased levels of transcripts of those metabolic genes.

The *D. melanogaster daw* Mutant and the Specialist *D. sechellia* Accumulate Various Common Metabolites on the Carbohydrate-Rich Diet

Previous studies have shown that overexpression of TCA cycle enzyme genes cause increases in production of intermediates (Anoop et al., 2003; Ghosh and O'Connor, 2014; Koyama et al., 2000; Tesfaye et al., 2001). To examine whether the differences in metabolic gene regulation among the species impact their metabolism, we performed GC-MS-based metabolomic analysis using wandering male larvae. In the wild-type *D. melanogaster*, most metabolites did not change between the diets (Figure 6A), and only 4 metabolites were significantly increased on the M diet (Figures 6B and 6C; Table S7). In contrast, the *daw* mutants increased 54 metabolites on the M diet, most of which are intermediates of metabolic pathways catalyzed by

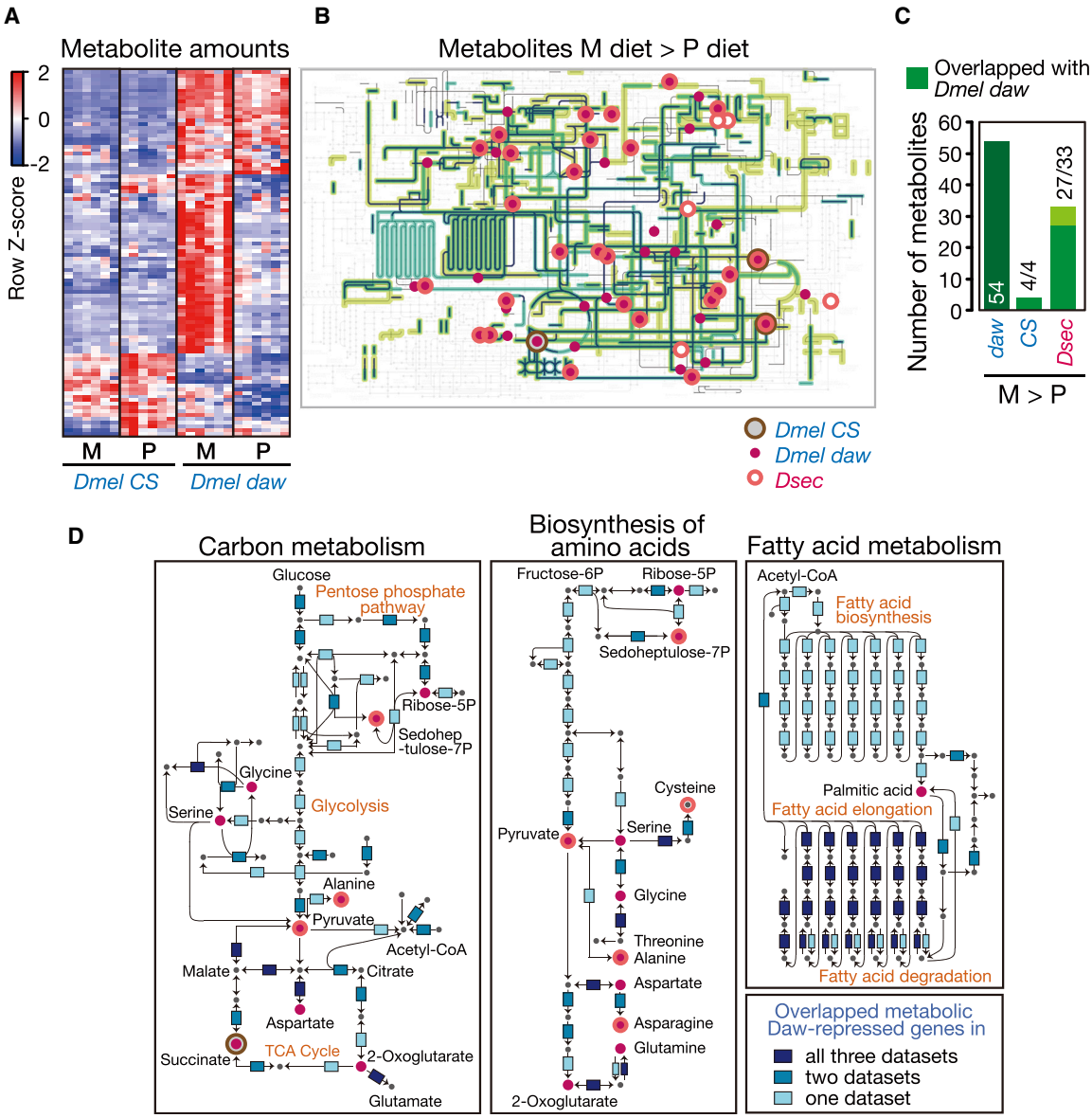

Figure 6. The *D. melanogaster daw* Mutant and the Specialist *D. sechellia* Accumulate Various Common Metabolites on the Carbohydrate-Rich Diet

(A) A heatmap showing relative abundance of metabolites in the wild-type *D. melanogaster CS* and the *daw* mutant.

(B) Mapping of significantly increased metabolites on the M diet compared to the P diet, to metabolic pathways. Not all of the increased metabolites were mapped. See also Table S7.

(C) Number of increased metabolites on the M diet compared to the P diet and the number that overlaps with the *daw* mutants.

(D) Representative metabolic pathways catalyzed by the Daw-repressed gene products in whole bodies or muscles of wandering third-instar larvae or whole bodies of first-instar larvae. Increased metabolites on the M diet compared to the P diet were also mapped as in (B).

See also Figures S5 and S6 and Tables S2, S3, S5, S6, and S7.

the Daw-repressed gene products (Figures 6A–6D; Table S7). Notably, 33 metabolites were increased in the specialist *D. sechellia* on the M diet, and these substantially overlapped with those that were increased in the *daw* mutant (27/33 metabolites; Figures 6B–6D; Table S7). We further investigated the effects of the diets on metabolism by observing lipid droplets in the fat body. In the wild-type *D. melanogaster*, larger lipid droplets are seen under much higher carbohydrate conditions than the M or C diet, and these findings have been discussed in the context of obesity (Musselman et al., 2011; Öst et al., 2014). In contrast to the wild-type *D. melanogaster*, in which the lipid droplet size did not significantly change between the M and the P diets, the *daw* mutant and *D. sechellia* increased the lipid droplet size on the M diet (Figure S6). These results imply that

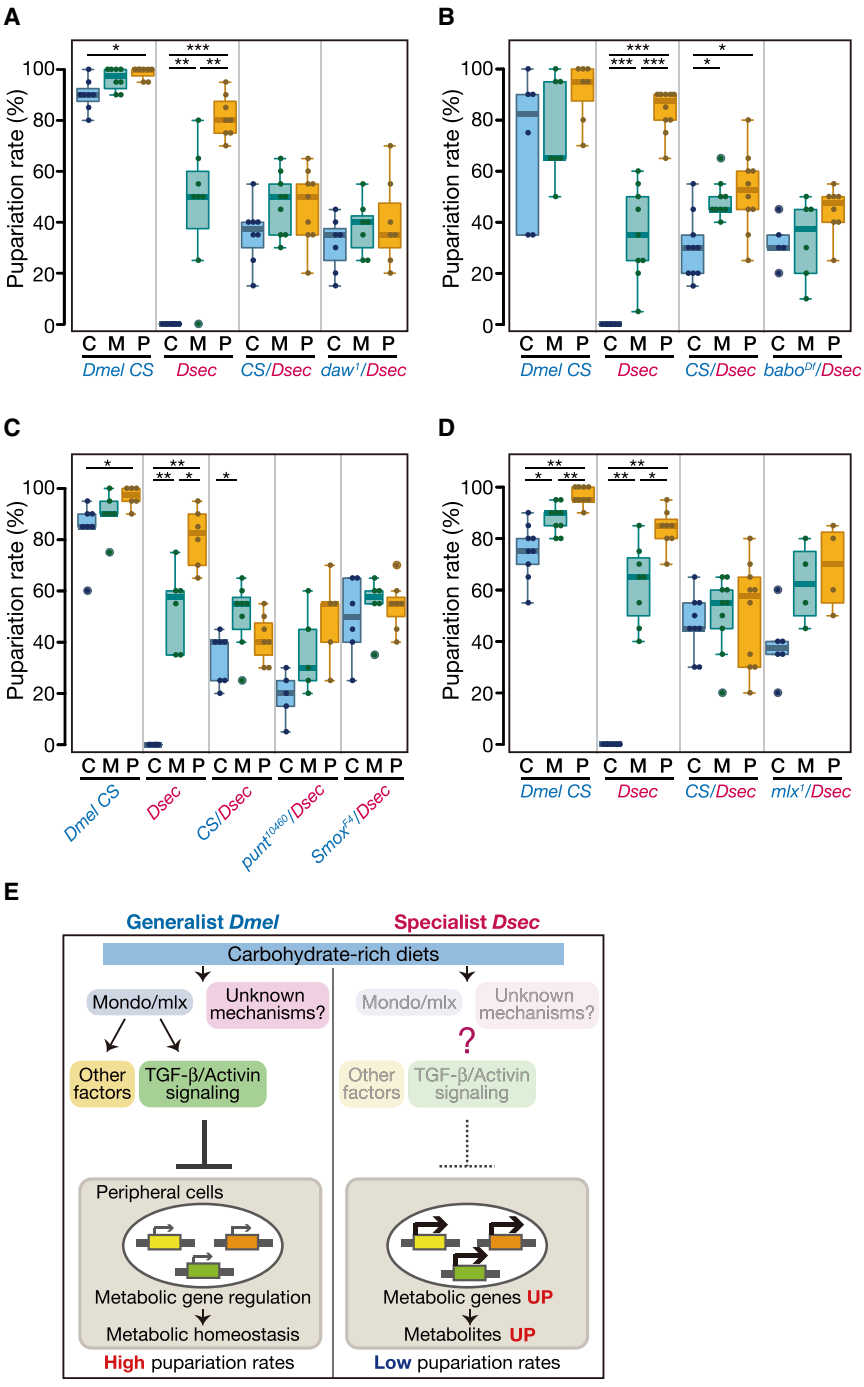

Figure 7. The Defect in the Specialist *D. sechellia* Cannot Be Attributed to a Single Gene Mutation of the Known Components or an Upstream Regulator of TGF-β/Activin Signaling

(A–D) Pupariation rates of the wild-type *D. melanogaster CS*, *D. sechellia*, hybrids between *D. melanogaster CS* and *D. sechellia* (*CS/Dsec*), and hybrids between *D. melanogaster* mutants of known components or an upstream regulator of TGF-β/Activin signaling and *D. sechellia*. Hybrids between *D. melanogaster daw* mutant and *D. sechellia* (daw^1/*Dsec*, A), hybrids between a *D. melanogaster* line with a deleted *babo* gene and *D. sechellia* ($babo^{Df}$/*Dsec*, B), hybrids between *D. melanogaster punt* mutants and *D. sechellia* ($punt^{10460}$/*Dsec*, C), hybrids between *D. melanogaster Smox* mutants and *D. sechellia* ($Smox^{F4}$/*Dsec*, C), and hybrids between *D. melanogaster mlx* mutants and *D. sechellia* (mlx^1/*Dsec*, D) were examined. Boxplots are depicted as in Figure 1D. *p < 0.05, **p < 0.01, and ***p < 0.001 (Steel-Dwass test). n = 7–9 (A), 5–10 (B), 5–8 (C), and 4–10 (D). To generate the hybrids, virgin female *D. melanogaster* were crossed to male *D. sechellia*. See also Figure S7.

(E) Summary of this study. A question mark (?) indicates hypothetical defects in carbohydrate-responsive mechanisms in the specialist.

their fat bodies are more sensitive to the load of carbohydrates than those of the wild-type *D. melanogaster* and that this phenotype may correlate with nutritional adaptability or lack thereof. Taken together, our results show that the specialists, especially *D. sechellia* and the *D. melanogaster daw* mutant, cannot coordinately control the amounts of metabolites and severely compromises adaptation on the carbohydrate-rich diets, whereas the wild-type *D. melanogaster* can maintain metabolic homeostasis and successfully adapts to the diets (Figure 7E).

Our results highlight phenotypic similarities between the specialists *D. sechellia* and *D. elegans* and the generalist *D. melanogaster daw* mutants, which imply the possibility that the carbohydrate-driven differences in gene expression come about by retention of gene regulation by the TGF-β/Activin signaling pathway in the generalists and its defect or loss in the specialists *D. sechellia* and *D. elegans*. Previous studies have shown that *D. sechellia* evolved from the generalists and underwent accelerated chemoreceptor gene loss compared to the generalists (Hey and Kliman, 1993; Kliman et al., 2000; McBride, 2007; McBride et al., 2007). We assessed whether *D. sechellia* also lost some gene functions in the carbohydrate-adaptive system by generating hybrids between *D. sechellia* and *D. melanogaster* mutants of the known components or an upstream regulator of TGF-β/Activin signaling. However, they were still able to develop on the carbohydrate-rich diets (Figures 7A–7D and S7). This result suggests that the evolutionary changes in *D. sechellia* cannot be attributed to a single gene mutation of the genes tested, but rather may be caused by multiple loci associated with TGF-β/Activin signaling. An alternative interpretation of our results of the hybrid analyses would be that the specialists *D. sechellia* and *D. elegans* lost carbohydrate-responsive system(s) other than TGF-β/Activin signaling

(Figure 7E). We further discuss our results, including these possibilities, below.

DISCUSSION

Collectively, our results have strongly suggested that robust carbohydrate-responsive regulation of gene expression and metabolism contribute to strong nutritional adaptability of the generalist species during development. One possible interpretation of our results from hybrids between *D. sechellia* and *D. melanogaster* is that the defect in the specialist *D. sechellia* could be caused by multiple loci associated with TGF-β/Activin signaling. This speculation is consistent with previous studies suggesting that large- and smaller-effect loci in *D. sechellia* contribute to toxin resistance additively (Huang and Erezyilmaz, 2015; Jones, 1998). Indeed, many studies in *D. melanogaster* and the laboratory mouse *Mus musculus* have shown that (1) complex traits are affected by multiple interacting loci with individually small and environmentally sensitive effects and (2) many sequence variations are located in intergenic regions, probably impacting regulatory mechanisms, thereby altering gene expression (Flint and Mackay, 2009; Mackay, 2009).

Although the phenotypic similarities between the specialists *D. sechellia* and *D. elegans* and the generalist *D. melanogaster daw* mutants are intriguing, we have also found differences. For example, *D. sechellia* exhibited a more severe unadaptability phenotype than the *daw* mutants. More than 80% of *D. sechellia* larvae died at the first-instar stage, and less than 10% of the larvae developed to the second-instar stage on the C diet, whereas more than 30% of the *daw* mutants developed to the second-instar stage (Figures 1F and 3D). In addition, many of the expression values of the metabolic Daw-repressed genes were markedly higher in *D. sechellia* compared to the *daw* mutant in muscles at the wandering third-instar stage and in the whole body of the first-instar stage (Figures 5B and 5D). These results raise the possibility that *D. sechellia* may have additional defects in other regulatory mechanisms, including unidentified adaptive systems, associated with or distinct from TGF-β/Activin signaling (Figure 7E; see also a caveat in "Designs for interspecies and omics analyses" in STAR Methods). Furthermore, there was also a difference between the two *D. melanogaster* mutants, *mlx* and *daw*. The *mlx* mutant failed to adapt to not only the C diet but also the M diet (Figure 3B), which is a more severe phenotype than that of the *daw* mutant (Figure 3A) and the two specialists *D. sechellia* and *D. elegans* (Figure 1D). This result implies the presence of other factors for adaptation that are downstream of Mlx and separate from TGF-β/Activin signaling ("Other factors" in Figure 7E). To unravel the causative step(s) and genetic architecture of distinct nutritional adaptabilities in the specialists *D. sechellia* and *D. elegans* to the carbohydrate-rich diets, further studies focused on genomic differences associated with the distinct carbohydrate-responsive regulation will be needed. Recently, a phenotype-based introgression approach using hybrids between *D. simulans* and *D. sechellia* identified genomic regions in the generalist *D. simulans* that were sufficient for sugar tolerance (Melvin et al., 2018). This raises the possibility that these regions contain the responsible loci for the carbohydrate response of the generalists revealed in our study. Future research should elucidate the precise defects in the specialists and also investigate the possible interactions between TGF-β/Activin signaling and genes for other regulatory mechanisms, including those in the genomic regions identified in the aforementioned study.

Our interspecies comparative analyses revealed phenotypic similarities and differences even among the three specialists. The phenotypes of *D. sechellia* and *D. elegans* were similar to each other with regard to adaptability to the C, M, and P diets (Figure 1D) and carbohydrate-responsive profiles of gene expression (Figures 4B and 4C), but they differed with regard to the critical timings of lethality on the C diet (Figure 1F), metabolic profiles (Table S7), and adaptation to the M diet with PA (Figure 3F). Considering these results and phylogenetic analyses showing independent evolutionary histories of *D. sechellia* and *D. elegans* on their particular respective hosts (Chen et al., 2014), these two specialists are quite likely to have incurred different mutations responsible for loss of the carbohydrate-adaptive systems. Our study supports an important possibility of a genome-environment interaction: the two specialists *D. sechellia* and *D. elegans* independently lost the carbohydrate-adaptive systems, which became superfluous during evolution in the constant low-carbohydrate environments. We also found that nutritional adaptability of the specialist *D. erecta* was different from those of the generalists or the two other specialist species, *D. sechellia* and *D. elegans.* The specialist *D. erecta* developed well on the M diet but incurred severely reduced pupariation rates on both the C and the P diets (Figure 1D). Our whole-body RNA-seq data also showed that dietary responses of *D. erecta* were distinct from those of the generalists or the two other specialist species. As for the Daw-activated genes, dietary responses of *D. erecta* were closer to those of the specialist *D. sechellia*, *D. elegans*, and *D. melanogaster daw* mutants (Figures 4B and 4C). On the other hand, as for the Daw-repressed genes, dietary responses of *D. erecta* were much closer to those of the generalists (Figures 4B and 4C). All of these results imply that *D. erecta* is defective in some regulatory mechanisms for nutritional adaptability other than TGF-β/Activin signaling. Interestingly, the P:C ratio of the food resource for *D. erecta* is located in the middle with respect to the widely varying resources for *D. melanogaster* (Figure 2F). The variation in nutritional adaptability among the specialist species might be attributed to differences in their feeding habits.

Various species in nature show complex adaptations to diverse environments, whose underlying mechanisms still remain to be elucidated. Our interspecies comparative study provides a powerful approach to understand how environment-responsive systems function and how they can evolve through genome-environment interactions.

STAR★METHODS

Detailed methods are provided in the online version of this paper and include the following:

- KEY RESOURCES TABLE
- LEAD CONTACT AND MATERIALS AVAILABILITY

SUPPLEMENTAL INFORMATION

Supplemental Information can be found online at https://doi.org/10.1016/j.celrep.2019.08.030.

ACKNOWLEDGMENTS

We thank T. Kondo and Y. Sando for performing RNA sequencing; the metabolomics core facility at the University of Utah and J. Cox for GC-MS analysis of larvae; D. Shibata, A. Kurabayashi, T. Kawada, and T. Kambe for critical advice about GC-MS analysis of fermented foods; T. Usui, T. Kondo, and J.A. Hejna for polishing the manuscript; and K. Tamura, I. Ohshima, T. Matsuo, S. Koshikawa, T. Nishimura, M. Umeda, T. Suito, B. Lemaitre, M.B. O'Connor, B. Oliver, Z. Chen, T. Takano, V.I. Hietakangas, and members of the Uemura laboratory for technical advice and discussions. This work was supported by AMED-CREST (JP18gm1110001 to T.U.); the Mitsubishi Foundation (to T.U.); the SPIRITS program of Kyoto University (to T.U.); the Japan Society for the Promotion of Science (JSPS; 15H02400 and 15K14524 to T.U., 15K18455 and 17K15039 to Y.H., and 16J10660 to K.W.); MEXT (17H05766 to T.U.); the Naito Foundation (to Y.H.); the Sasakawa Scientific Research Grant (to Y.H.); a grant for RNA sequencing from MEXT KAKENHI (221S0002); and the Cooperative Research Grant of the Genome Research for BioResource, NODAI Genome Research Center, Tokyo University of Agriculture.

AUTHOR CONTRIBUTIONS

Y.H. and T.U. conceived and designed the study. Y.H. and K.W. designed experiments. K.W. performed most of the experiments. Y.H. analyzed omics data and performed some initial experiments. K.W., Y.H., M.W., and T.U. collected wild *D. elegans* and morning glory. M.W. identified species of the generalists collected in the wild. Y.K. performed some experiments and quantifications of pupariation rate. S.M. performed the lipid droplet staining experiment and quantification. H.U. and S.Y. performed RNA sequencing (platform "N"). Y.H., K.W., and T.U. wrote and edited the manuscript, with contributions from all authors.

DECLARATION OF INTERESTS

The authors declare no competing interests.

Received: August 21, 2018
Revised: May 17, 2019
Accepted: August 6, 2019
Published: September 3, 2019

SUPPORTING CITATIONS

The following references appear in the Supplemental Information: Davis et al. (1997); DiAntonio et al. (1999); Ranganayakulu et al. (1996); Sievers et al. (2011); Wrana et al. (1994).

REFERENCES

Anagnostou, C., Dorsch, M., and Rohlfs, M. (2010). Influence of dietary yeasts on Drosophila melanogaster life-history traits. Entomol. Exp. Appl. *136*, 1–11.

Anders, S., McCarthy, D.J., Chen, Y., Okoniewski, M., Smyth, G.K., Huber, W., and Robinson, M.D. (2013). Count-based differential expression analysis of RNA sequencing data using R and Bioconductor. Nat. Protoc. *8*, 1765–1786.

Anders, S., Pyl, P.T., and Huber, W. (2015). HTSeq–a Python framework to work with high-throughput sequencing data. Bioinformatics *31*, 166–169.

Anoop, V.M., Basu, U., McCammon, M.T., McAlister-Henn, L., and Taylor, G.J. (2003). Modulation of citrate metabolism alters aluminum tolerance in yeast and transgenic canola overexpressing a mitochondrial citrate synthase. Plant Physiol. *132*, 2205–2217.

Awasaki, T., Huang, Y., O'Connor, M.B., and Lee, T. (2011). Glia instruct developmental neuronal remodeling through TGF-β signaling. Nat. Neurosci. *14*, 821–823.

Bai, H., Kang, P., Hernandez, A.M., and Tatar, M. (2013). Activin signaling targeted by insulin/dFOXO regulates aging and muscle proteostasis in Drosophila. PLoS Genet. *9*, e1003941.

Broderick, N.A., and Lemaitre, B. (2012). Gut-associated microbes of Drosophila melanogaster. Gut Microbes *3*, 307–321.

Brown, J.B., Boley, N., Eisman, R., May, G.E., Stoiber, M.H., Duff, M.O., Booth, B.W., Wen, J., Park, S., Suzuki, A.M., et al. (2014). Diversity and dynamics of the Drosophila transcriptome. Nature *512*, 393–399.

Chandler, J.A., Lang, J.M., Bhatnagar, S., Eisen, J.A., and Kopp, A. (2011). Bacterial communities of diverse Drosophila species: ecological context of a host-microbe model system. PLoS Genet. *7*, e1002272.

Chen, Z.X., Sturgill, D., Qu, J., Jiang, H., Park, S., Boley, N., Suzuki, A.M., Fletcher, A.R., Plachetzki, D.C., FitzGerald, P.C., et al. (2014). Comparative validation of the D. melanogaster modENCODE transcriptome annotation. Genome Res. *24*, 1209–1223.

Chng, W.A., Sleiman, M.S.B., Schüpfer, F., and Lemaitre, B. (2014). Transforming growth factor β/activin signaling functions as a sugar-sensing feedback loop to regulate digestive enzyme expression. Cell Rep. *9*, 336–348.

Clark, A.G., Eisen, M.B., Smith, D.R., Bergman, C.M., Oliver, B., Markow, T.A., Kaufman, T.C., Kellis, M., Gelbart, W., Iyer, V.N., et al.; Drosophila 12 Genomes Consortium (2007). Evolution of genes and genomes on the Drosophila phylogeny. Nature *450*, 203–218.

Cooper, K.W. (1950). Normal spermatogenesis in Drosophila. In Biology of Drosophila, M. Demerec, ed. (Wiley New York), pp. 1–61.

David, J.R., McEvey, S.F., and Tsacas, L. (1989). Drosophila communities on Mauritius and the ecological niche of D. mauritiana (Diptera, Drosophilidae). Rev. Zool. Africaine. J. Afr. Zool. *103*, 107–116.

Davis, G.W., Schuster, C.M., and Goodman, C.S. (1997). Genetic analysis of the mechanisms controlling target selection: target-derived Fasciclin II regulates the pattern of synapse formation. Neuron *19*, 561–573.

DiAntonio, A., Petersen, S.A., Heckmann, M., and Goodman, C.S. (1999). Glutamate receptor expression regulates quantal size and quantal content at the Drosophila neuromuscular junction. J. Neurosci. *19*, 3023–3032.

Dignan, C., Burlingame, B., Kumar, S., and Aalbersberg, W. (2004). The Pacific Islands Food Composition Tables (Food and Agriculture Organization of the United Nations).

Droujinine, I.A., and Perrimon, N. (2016). Interorgan Communication Pathways in Physiology: Focus on Drosophila. Annu. Rev. Genet. *50*, 539–570.

Flint, J., and Mackay, T.F.C. (2009). Genetic architecture of quantitative traits in mice, flies, and humans. Genome Res. *19*, 723–733.

Gesualdi, S.C., and Haerry, T.E. (2007). Distinct signaling of Drosophila Activin/TGF-beta family members. Fly (Austin) *1*, 212–221.

Ghosh, A.C., and O'Connor, M.B. (2014). Systemic Activin signaling independently regulates sugar homeostasis, cellular metabolism, and pH balance in Drosophila melanogaster. Proc. Natl. Acad. Sci. USA *111*, 5729–5734.

Gibson, J.B., May, T.W., and Wilks, A.V. (1981). Genetic variation at the alcohol dehydrogenase locus in Drosophila melanogaster in relation to environmental variation: Ethanol levels in breeding sites and allozyme frequencies. Oecologia *51*, 191–198.

Greenfield, H., and Southgate, D.A.T. (2003). Food Composition Data: Production, Management, and Use, Second Edition (Food and Agriculture Organization of the United Nations).

Havula, E., Teesalu, M., Hyötyläinen, T., Seppälä, H., Hasygar, K., Auvinen, P., Orešič, M., Sandmann, T., and Hietakangas, V. (2013). Mondo/ChREBP-Mlx-regulated transcriptional network is essential for dietary sugar tolerance in Drosophila. PLoS Genet. *9*, e1003438.

Hey, J., and Kliman, R.M. (1993). Population genetics and phylogenetics of DNA sequence variation at multiple loci within the Drosophila melanogaster species complex. Mol. Biol. Evol. *10*, 804–822.

Hirai, Y., and Kimura, M.T. (1997). Incipient reproductive isolation between two morphs of Drosophila elegans (Diptera: Drosophilidae). Biol. J. Linn. Soc. Lond. *61*, 501–513.

Hu, T.T., Eisen, M.B., Thornton, K.R., and Andolfatto, P. (2013). A second-generation assembly of the Drosophila simulans genome provides new insights into patterns of lineage-specific divergence. Genome Res. *23*, 89–98.

Huang, Y., and Erezyilmaz, D. (2015). The Genetics of Resistance to Morinda Fruit Toxin During the Postembryonic Stages in Drosophila sechellia. G3 (Bethesda) *5*, 1973–1981.

Huang, W., Sherman, B.T., and Lempicki, R.A. (2009). Systematic and integrative analysis of large gene lists using DAVID bioinformatics resources. Nat. Protoc. *4*, 44–57.

Hulsen, T., de Vlieg, J., and Alkema, W. (2008). BioVenn - a web application for the comparison and visualization of biological lists using area-proportional Venn diagrams. BMC Genomics *9*, 488.

Johnson, R.N., O'Meally, D., Chen, Z., Etherington, G.J., Ho, S.Y.W., Nash, W.J., Grueber, C.E., Cheng, Y., Whittington, C.M., Dennison, S., et al. (2018). Adaptation and conservation insights from the koala genome. Nat. Genet. *50*, 1102–1111.

Jones, C.D. (1998). The genetic basis of Drosophila sechellia's resistance to a host plant toxin. Genetics *149*, 1899–1908.

Kanehisa, M., Goto, S., Sato, Y., Furumichi, M., and Tanabe, M. (2012). KEGG for integration and interpretation of large-scale molecular data sets. Nucleic Acids Res. *40*, D109–D114.

Kanehisa, M., Furumichi, M., Tanabe, M., Sato, Y., and Morishima, K. (2017). KEGG: new perspectives on genomes, pathways, diseases and drugs. Nucleic Acids Res. *45* (*D1*), D353–D361.

Kim, D., Pertea, G., Trapnell, C., Pimentel, H., Kelley, R., and Salzberg, S.L. (2013). TopHat2: accurate alignment of transcriptomes in the presence of insertions, deletions and gene fusions. Genome Biol. *14*, R36.

Kliman, R.M., Andolfatto, P., Coyne, J.A., Depaulis, F., Kreitman, M., Berry, A.J., McCarter, J., Wakeley, J., and Hey, J. (2000). The population genetics of the origin and divergence of the Drosophila simulans complex species. Genetics *156*, 1913–1931.

Koyama, H., Kawamura, A., Kihara, T., Hara, T., Takita, E., and Shibata, D. (2000). Overexpression of mitochondrial citrate synthase in Arabidopsis thaliana improved growth on a phosphorus-limited soil. Plant Cell Physiol. *41*, 1030–1037.

Lang, M., Murat, S., Clark, A.G., Gouppil, G., Blais, C., Matzkin, L.M., Guittard, E., Yoshiyama-Yanagawa, T., Kataoka, H., Niwa, R., et al. (2012). Mutations in the neverland gene turned Drosophila pachea into an obligate specialist species. Science *337*, 1658–1661.

Langerak, S., Kim, M.-J., Lamberg, H., Godinez, M., Main, M., Winslow, L., O'Connor, M.B., and Zhu, C.C. (2018). The *Drosophila* TGF-beta/Activin-like ligands Dawdle and Myoglianin appear to modulate adult lifespan through regulation of 26S proteasome function in adult muscle. Biol. Open *7*, bio029454.

Langmead, B., and Salzberg, S.L. (2012). Fast gapped-read alignment with Bowtie 2. Nat. Methods *9*, 357–359.

Lassmann, T., Hayashizaki, Y., and Daub, C.O. (2009). TagDust–a program to eliminate artifacts from next generation sequencing data. Bioinformatics *25*, 2839–2840.

Lavista-Llanos, S., Svatoš, A., Kai, M., Riemensperger, T., Birman, S., Stensmyr, M.C., and Hansson, B.S. (2014). Dopamine drives Drosophila sechellia adaptation to its toxic host. eLife *3*, e03785.

Lee, K.P., Simpson, S.J., Clissold, F.J., Brooks, R., Ballard, J.W.O., Taylor, P.W., Soran, N., and Raubenheimer, D. (2008). Lifespan and reproduction in Drosophila: New insights from nutritional geometry. Proc. Natl. Acad. Sci. USA *105*, 2498–2503.

Lehmann, R., and Nüsslein-Volhard, C. (1986). Abdominal segmentation, pole cell formation, and embryonic polarity require the localized activity of oskar, a maternal gene in Drosophila. Cell *47*, 141–152.

Li, H., Handsaker, B., Wysoker, A., Fennell, T., Ruan, J., Homer, N., Marth, G., Abecasis, G., and Durbin, R.; 1000 Genome Project Data Processing Subgroup (2009). The Sequence Alignment/Map format and SAMtools. Bioinformatics *25*, 2078–2079.

Linz, J., Baschwitz, A., Strutz, A., Dweck, H.K.M., Sachse, S., Hansson, B.S., and Stensmyr, M.C. (2013). Host plant-driven sensory specialization in Drosophila erecta. Proc. Biol. Sci. *280*, 20130626.

Loraine, A.E., Blakley, I.C., Jagadeesan, S., Harper, J., Miller, G., and Firon, N. (2015). Analysis and visualization of RNA-Seq expression data using RStudio, Bioconductor, and Integrated Genome Browser. Methods Mol. Biol. *1284*, 481–501.

Mackay, T.F.C. (2009). The genetic architecture of complex behaviors: lessons from Drosophila. Genetica *136*, 295–302.

Markow, T.A. (2015). The secret lives of Drosophila flies. eLife *4*, 1–9.

Markow, T.A., and O'Grady, P. (2005). Drosophila: A Guide to Species Identification and Use (Elsevier).

Markow, T.A., and O'Grady, P. (2008). Reproductive ecology of *Drosophila*. Funct. Ecol. *22*, 747–759.

Matavelli, C., Carvalho, M.J.A., Martins, N.E., and Mirth, C.K. (2015). Differences in larval nutritional requirements and female oviposition preference reflect the order of fruit colonization of Zaprionus indianus and Drosophila simulans. J. Insect Physiol. *82*, 66–74.

Matsuo, T., Sugaya, S., Yasukawa, J., Aigaki, T., and Fuyama, Y. (2007). Odorant-binding proteins OBP57d and OBP57e affect taste perception and host-plant preference in Drosophila sechellia. PLoS Biol. *5*, e118.

Mattila, J., Havula, E., Suominen, E., Teesalu, M., Surakka, I., Hynynen, R., Kilpinen, H., Väänänen, J., Hovatta, I., Käkelä, R., et al. (2015). Mondo-Mlx Mediates Organismal Sugar Sensing through the Gli-Similar Transcription Factor Sugarbabe. Cell Rep. *13*, 350–364.

Matzkin, L.M., Johnson, S., Paight, C., Bozinovic, G., and Markow, T.A. (2011). Dietary protein and sugar differentially affect development and metabolic pools in ecologically diverse Drosophila. J. Nutr. *141*, 1127–1133.

McBride, C.S. (2007). Rapid evolution of smell and taste receptor genes during host specialization in Drosophila sechellia. Proc. Natl. Acad. Sci. USA *104*, 4996–5001.

McBride, C.S., Arguello, J.R., and O'Meara, B.C. (2007). Five Drosophila genomes reveal nonneutral evolution and the signature of host specialization in the chemoreceptor superfamily. Genetics *177*, 1395–1416.

McCarthy, D.J., Chen, Y., and Smyth, G.K. (2012). Differential expression analysis of multifactor RNA-Seq experiments with respect to biological variation. Nucleic Acids Res. *40*, 4288–4297.

Melvin, R.G., Lamichane, N., Havula, E., Kokki, K., Soeder, C., Jones, C.D., and Hietakangas, V. (2018). Natural variation in sugar tolerance associates

with changes in signaling and mitochondrial ribosome biogenesis. eLife *7*, 1–10.

Musselman, L.P., Fink, J.L., Narzinski, K., Ramachandran, P.V., Hathiramani, S.S., Cagan, R.L., and Baranski, T.J. (2011). A high-sugar diet produces obesity and insulin resistance in wild-type Drosophila. Dis. Model. Mech. *4*, 842–849.

Nazario-Yepiz, N.O., Loustalot-Laclette, M.R., Carpinteyro-Ponce, J., Abreu-Goodger, C., and Markow, T.A. (2017). Transcriptional responses of ecologically diverse Drosophila species to larval diets differing in relative sugar and protein ratios. PLoS ONE *12*, e0183007.

Neph, S., Kuehn, M.S., Reynolds, A.P., Haugen, E., Thurman, R.E., Johnson, A.K., Rynes, E., Maurano, M.T., Vierstra, J., Thomas, S., et al. (2012). BEDOPS: high-performance genomic feature operations. Bioinformatics *28*, 1919–1920.

Niwa, R., Namiki, T., Ito, K., Shimada-Niwa, Y., Kiuchi, M., Kawaoka, S., Kayukawa, T., Banno, Y., Fujimoto, Y., Shigenobu, S., et al. (2010). Non-molting glossy/shroud encodes a short-chain dehydrogenase/reductase that functions in the 'Black Box' of the ecdysteroid biosynthesis pathway. Development *137*, 1991–1999.

Okamoto, N., Yamanaka, N., Yagi, Y., Nishida, Y., Kataoka, H., O'Connor, M.B., and Mizoguchi, A. (2009). A fat body-derived IGF-like peptide regulates postfeeding growth in Drosophila. Dev. Cell *17*, 885–891.

Öst, A., Lempradl, A., Casas, E., Weigert, M., Tiko, T., Deniz, M., Pantano, L., Boenisch, U., Itskov, P.M., Stoeckius, M., et al. (2014). Paternal diet defines offspring chromatin state and intergenerational obesity. Cell *159*, 1352–1364.

Peterson, A.J., Jensen, P.A., Shimell, M., Stefancsik, R., Wijayatonge, R., Herder, R., Raftery, L.A., and O'Connor, M.B. (2012). R-Smad competition controls activin receptor output in Drosophila. PLoS ONE *7*, e36548.

Piper, M.D.W., Blanc, E., Leitão-Gonçalves, R., Yang, M., He, X., Linford, N.J., Hoddinott, M.P., Hopfen, C., Soultoukis, G.A., Niemeyer, C., et al. (2014). A holidic medium for Drosophila melanogaster. Nat. Methods *11*, 100–105.

R Core Team (2017). R: A Language and Environment for Statistical Computing, R Foundation for Statistical Computing (Vienna, Austria).

R'Kha, S., Moreteau, B., Coyne, J.A., and David, J.R. (1997). Evolution of a lesser fitness trait: egg production in the specialist Drosophila sechellia. Genet. Res. *69*, 17–23.

R'Kha, S., Capy, P., and David, J.R. (1991). Host-plant specialization in the Drosophila melanogaster species complex: a physiological, behavioral, and genetical analysis. Proc. Natl. Acad. Sci. U S A. *88*, 1835–1839.

Rachkeeree, A., Kantadoung, K., Suksathan, R., Puangpradab, R., Page, P.A., and Sommano, S.R. (2018). Nutritional Compositions and Phytochemical Properties of the Edible Flowers from Selected Zingiberaceae Found in Thailand. Front. Nutr. *5*, 3.

Ranganayakulu, G., Schulz, R.A., and Olson, E.N. (1996). Wingless signaling induces nautilus expression in the ventral mesoderm of the Drosophila embryo. Dev. Biol. *176*, 143–148.

Rio, B., Couturier, G., Lemeunier, F., and Lachaise, D. (1983). Evolution d'une spécialisation saisonière chez Drosophila erecta (Dipt., Drosophilidae). Ann. Soc. Entomol. Fr. *19*, 235–248.

Robinson, M.D., McCarthy, D.J., and Smyth, G.K. (2010). edgeR: a Bioconductor package for differential expression analysis of digital gene expression data. Bioinformatics *26*, 139–140.

Ryu, J.H., Kim, S.H., Lee, H.Y., Bai, J.Y., Nam, Y.D., Bae, J.W., Lee, D.G., Shin, S.C., Ha, E.M., and Lee, W.J. (2008). Innate immune homeostasis by the homeobox gene caudal and commensal-gut mutualism in Drosophila. Science *319*, 777–782.

Serpe, M., and O'Connor, M.B. (2006). The metalloprotease tolloid-related and its TGF-β-like substrate Dawdle regulate Drosophila motoneuron axon guidance. Development *133*, 4969–4979.

Sievers, F., Wilm, A., Dineen, D., Gibson, T.J., Karplus, K., Li, W., Lopez, R., McWilliam, H., Remmert, M., Söding, J., et al. (2011). Fast, scalable generation of high-quality protein multiple sequence alignments using Clustal Omega. Mol. Syst. Biol. *7*, 539.

Simpson, S.J., Le Couteur, D.G., and Raubenheimer, D. (2015). Putting the balance back in diet. Cell *161*, 18–23.

Solon-Biet, S.M., McMahon, A.C., Ballard, J.W.O., Ruohonen, K., Wu, L.E., Cogger, V.C., Warren, A., Huang, X., Pichaud, N., Melvin, R.G., et al. (2014). The ratio of macronutrients, not caloric intake, dictates cardiometabolic health, aging, and longevity in ad libitum-fed mice. Cell Metab. *19*, 418–430.

Tee, E.S., Noor, M.I., Azudin, M.N., and Idris, K.I. (1997). Nutrient Composition of Malaysian Foods, Fourth Edition (Kuala Lumpur, Malaysia: Institute for Medical Research).

Tennessen, J.M., Barry, W.E., Cox, J., and Thummel, C.S. (2014). Methods for studying metabolism in Drosophila. Methods *68*, 105–115.

Tesfaye, M., Temple, S.J., Allan, D.L., Vance, C.P., and Samac, D.A. (2001). Overexpression of malate dehydrogenase in transgenic alfalfa enhances organic acid synthesis and confers tolerance to aluminum. Plant Physiol. *127*, 1836–1844.

Tsacas, L., and Bächli, G. (1981). Drosophila sechellia. n. sp., huitième espèce du sous-groupe melanogaster des iles Séchelles (Diptera, Drosophilidae). Rev. Fr. d'Entomologie *3*, 146–150.

US Department of Agriculture Agricultural Research Service Nutrient Data Laboratory (2018). USDA National Nutrient Database for Standard Reference. https://ndb.nal.usda.gov/ndb/.

Waterhouse, R.M., Zdobnov, E.M., Tegenfeldt, F., Li, J., and Kriventseva, E.V. (2011). OrthoDB: the hierarchical catalog of eukaryotic orthologs in 2011. Nucleic Acids Res. *39*, D283–D288.

Worley, B., and Powers, R. (2013). Multivariate Analysis in Metabolomics. Curr. Metabolomics *1*, 92–107.

Wrana, J.L., Attisano, L., Wieser, R., Ventura, F., and Massagué, J. (1994). Mechanism of activation of the TGF-β receptor. Nature *370*, 341–347.

Xi, B., Gu, H., Baniasadi, H., and Raftery, D. (2014). Statistical analysis and modeling of mass spectrometry-based metabolomics data. In Mass Spectrometry in Metabolomics: Methods and Protocols, D. Raftery, ed. (Springer New York), pp. 333–353.

Xia, J., Sinelnikov, I.V., Han, B., and Wishart, D.S. (2015). MetaboAnalyst 3.0–making metabolomics more meaningful. Nucleic Acids Res. *43* (*W1*), W251–W257.

Yamada, R., Deshpande, S.A., Bruce, K.D., Mak, E.M., and Ja, W.W. (2015). Microbes Promote Amino Acid Harvest to Rescue Undernutrition in Drosophila. Cell Rep. *10*, 865–872.

Zhan, S., Merlin, C., Boore, J.L., and Reppert, S.M. (2011). The monarch butterfly genome yields insights into long-distance migration. Cell *147*, 1171–1185.

Zheng, X., Wang, J., Haerry, T.E., Wu, A.Y.-H., Martin, J., O'Connor, M.B., Lee, C.-H.J., and Lee, T. (2003). TGF-β signaling activates steroid hormone receptor expression during neuronal remodeling in the Drosophila brain. Cell *112*, 303–315.

STAR★METHODS

KEY RESOURCES TABLE

REAGENT or RESOURCE	SOURCE	IDENTIFIER
Chemicals, Peptides, and Recombinant Proteins		
Active dry yeast	Genesee Scientific	Cat#62-103
Yellow cornmeal	Genesee Scientific	Cat#62-100
Sucrose	WAKO	Cat#196-00015; CAS: 57-50-1
Propionic acid	Nacalai Tesque, Inc.	Cat#29018-55; CAS: 79-09-4
Butyl p-hydroxybenzoate	Nacalai Tesque, Inc.	Cat#06327-02; CAS: 94-26-8
Brilliant Blue FCF	WAKO	CAT#027-12842; CAS: 3844-45-9
RNase-Free DNase Set	QIAGEN	Cat#79254
Nile Red for microscopy	Sigma-Aldrich	Cat# 72485; CAS: 7385-67-3
VECTASHIELD Mounting Medium with DAPI	Vector Laboratories	Cat#H-1200
Critical Commercial Assays		
TRIzol Reagent	Invitrogen	Cat#15596018
RNeasy Mini Kit	QIAGEN	Cat#74104
ReverTra Ace qPCR RT Kit	TOYOBO	Cat#FSQ-101
THUNDERBIRD SYBR qPCR Mix	TOYOBO	Cat#QPS-201
Deposited Data		
GC-MS dataset of natural food resources	This paper	Table S1
RNA-seq datasets	This paper	Tables S2, S3, S4, S5, and S6; DDBJ: DRA004295, DRA006831, DRA007810 (BioProject # PRJDB4481)
GC-MS dataset of whole larvae	This paper	Table S7
Experimental Models: Organisms/Strains		
D. melanogaster: *Canton-S*	EHIME-Fly *Drosophila* Stocks of Ehime University	E-10002
D. simulans: wild type (genome strain)	Clark et al., 2007; KYORIN-Fly Fly Stocks of Kyorin University	K-S05; Tucson:14021- 0251.194
D. sechellia: wild type (genome strain)	Clark et al., 2007; KYORIN-Fly Fly Stocks of Kyorin University	K-S10; Tucson:14021-0248.25
D. elegans: wild type (genome strain)	Chen et al., 2014; EHIME-Fly *Drosophila* Stocks of Ehime University	HK0461.03; Tucson:14027-0461.03
D. erecta: wild type (genome strain)	Clark et al., 2007; KYORIN-Fly Fly Stocks of Kyorin University	K-S02; Tucson:14021-0224.01
D. melanogaster: daw^{1}/*CyO-GFP*	Gesualdi and Haerry, 2007	N/A
D. melanogaster: daw^{11}/*CyO-GFP*	Serpe and O'Connor, 2006	N/A
D. melanogaster: $babo^{DF6090}$/*CyO-act-GFP*	Zheng et al., 2003	N/A
D. melanogaster: $Smox^{F4}$/*FM7-act-GFP*	Peterson et al., 2012	N/A
D. melanogaster: mlx^{1}/*TM3-GFP*	Havula et al., 2013	N/A
D. melanogaster: *UAS-babo-c-miRNA*	Awasaki et al., 2011	RRID: BDSC_44402
D. melanogaster: osk^{301}/*TM3*	Lehmann and Nüsslein-Volhard, 1986	N/A
D. melanogaster: w^{-}; osk^{301}/*TM3*	Lehmann and Nüsslein-Volhard, 1986	N/A
D. melanogaster: *da-Gal4*	Bloomington *Drosophila* Stock Center	RRID: BDSC_55849
D. melanogaster: *Mef2-Gal4*	Bloomington *Drosophila* Stock Center	RRID: BDSC_27390
D. melanogaster: *Sxl-eGFP*	Bloomington *Drosophila* Stock Center	RRID:BDSC_24105
D. melanogaster: $punt^{10460}$/*TM3,Sb,Ser*	Bloomington *Drosophila* Stock Center	RRID:BDSC_11745

(*Continued on next page*)

Continued

REAGENT or RESOURCE	SOURCE	IDENTIFIER
Oligonucleotides		
CG31226 forward: GCTATCCTTGCTATCCTTGCG	This paper	N/A
CG31226 reverse: TCCGTTGTAGGGTCCAAAGC	This paper	N/A
CG31644 forward: ACACTTTACACAACAATCCGC	This paper	N/A
CG31644 reverse: GGAGGACAGGACGATAGGTA	This paper	N/A
rp49 forward: CAGTCGGATCGATATGCTAAGCTG	Sequence from Okamoto et al., 2009	N/A
rp49 reverse: TAACCGATGTTGGGCATCAGATAC	Sequence from Okamoto et al., 2009	N/A
Software and Algorithms		
R	R Core Team, 2017	https://www.r-project.org/
Axiovision v3.1 acquisition software	Carl Zeiss	N/A
ImageJ	NIH	https://imagej.nih.gov/ij/
MetaboAnalyst	Xia et al., 2015	https://www.metaboanalyst.ca/
gtf2bed (BEDOPS ver. 2.4.12)	Neph et al., 2012	https://bedops.readthedocs.io/en/latest/
UCSC Genome Browser liftOver tool	N/A	https://genome-store.ucsc.edu/
TagDust (ver. 1.13)	Lassmann et al., 2009	http://tagdust.sourceforge.net/
Fastx-toolkit (ver. 0.0.14)	N/A	http://hannonlab.cshl.edu/fastx_toolkit/
Tophat ver. 2.0.13	Kim et al., 2013	https://ccb.jhu.edu/software/tophat/index.shtml
Bowtie2 ver. 2.2.3.0	Langmead and Salzberg, 2012	http://bowtie-bio.sourceforge.net/bowtie2/index.shtml
SAMtools ver. 1.1	Li et al., 2009	http://www.htslib.org/
htseq-count ver. 0.6.1p1	Anders et al., 2015	https://htseq.readthedocs.io/en/release_0.11.1/
edgeR Bioconductor package ver. 3.10.2	McCarthy et al., 2012; Robinson et al., 2010	https://bioconductor.org/packages/release/bioc/html/edgeR.html
KEGG Mapper Search&Color Pathway tool	Kanehisa et al., 2012	https://www.genome.jp/kegg/tool/map_pathway2.html
BioVenn	Hulsen et al., 2008	http://www.biovenn.nl/

LEAD CONTACT AND MATERIALS AVAILABILITY

Further information and requests for resources and reagents should be directed to and will be fulfilled by the Lead Contact, Yukako Hattori (yhattori@lif.kyoto-u.ac.jp). This study did not generate new unique reagents.

EXPERIMENTAL MODEL AND SUBJECT DETAILS

Drosophila strains and fly culture

D. melanogaster wild-type *Canton-S* (E-10002) and *D. elegans* (HK0461.03) were obtained from EHIME-Fly *Drosophila* Stocks of Ehime University. *D. simulans* (K-S05), *D. sechellia* (K-S10), and *D. erecta* (K-S02) were obtained from KYORIN-Fly Fly Stocks of Kyorin University. The following *D. melanogaster* lines were also used in this study: daw^{1}/*CyO-GFP*, daw^{11}/*CyO-GFP*, $babo^{DF6090}$/*CyO-act-GFP*, and $Smox^{F4}$/*FM7-act-GFP* were gifts from M. B. O'Connor (Gesualdi and Haerry, 2007; Peterson et al., 2012; Serpe and O'Connor, 2006; Zheng et al., 2003). mlx^{1}/*TM3-GFP* was a gift from V. Hietakangas (Havula et al., 2013). *UAS-babo-c-miRNA* was a gift from T. Awasaki (Awasaki et al., 2011). osk^{301}/*TM3* and w^{-}; osk^{301}/*TM3* were gifts from A. Nakamura (Lehmann and Nüsslein-Volhard, 1986). *da-Gal4* (#55849), *Mef2-Gal4* (#27390), *Sxl-eGFP* (# 24105), $punt^{10460}$/*TM3,Sb,Ser* (#11745) were obtained from Bloomington *Drosophila* Stock Center. The genotype of the *D. melanogaster daw* mutant was $daw^{1/11}$, unless described otherwise.

All stocks were maintained at 25°C on a laboratory standard food containing, per liter of water, 51 g of corn flour, 26 g of corn grits (NIPPN), 44 g of dry yeast (Asahi Food & Healthcare, Y2A), 110 g of glucose (Kato Kagaku, Fuji Crystar), 8 g of agar (Matsuki Kanten), 2.9 mL of propionic acid (Nacalai, #29018-55), and 2.9 mL of 10% butyl p-hydroxybenzoate (Nacalai, #06327-02; diluted in 70% ethanol).

METHOD DETAILS

Experimental diets

We mainly used three isocaloric diets that differ in protein-to-carbohydrate (P:C) ratios as described previously (Matzkin et al., 2011), with the modification of the amounts of yeast, sucrose, and antifungal agents (propionic acid and butyl p-hydroxybenzoate): C diet

(high-carbohydrate diet), M diet (medium diet), and P diet (high-protein or high-yeast diet). The P:C ratio of the M diet is close to that of our standard food above. All of the C, M, and P diets were composed of active dry yeast (Genesee Scientific, #62-103), sucrose (WAKO, #196-00015), yellow cornmeal (Genesee Scientific, # 62-100), and agar (Matsuki Kanten). The complete compositions of these diets can be found in Table S1A. After ingredients were mixed with 200 mL water, they were boiled and stirred for 4 min. Once the foods were cooled down, 0.6 mL propionic acid (Nacalai, #29018-55) and 2 mL 10% butyl p-hydroxybenzoate (Nacalai, #06327-02) in 70% ethanol were added. These foods were dispensed to vials and left for one day before use. When we measured pupariation rates of first instar larvae on different diets, these foods in vials were mashed and about 1.2 mL volume was put into each 1.5 mL tube, using a 50 mL syringe (TERUMO), unless mentioned otherwise. Calculations of protein and carbohydrate (Figure 1B; Table S1A) and fat contents were based on the manufacturers' datasheets and Musselman et al. (2011).

Preparation of first instar larvae

To obtain larvae for our experiments, sexually mature adults were placed on apple agar plates [22.5 g of Bacto agar (Becton Dickinson, #214010), 500 mL of apple juice (KIRIN), and 500 mL of water] with yeast paste [dry yeast (Oriental Yeast) kneaded with water] and allowed to oviposit for 24 hr, unless otherwise mentioned. Embryos/larvae on these plates were washed with 0.7% NaCl + 0.3% Triton X-100 and collected through 70 μm Cell Strainers (Falcon, #352350). Newly hatched first instar larvae were collected and placed in 1.5 mL tubes (20 larvae/tube) or vials (200 larvae/vial) of each diet and incubated at 25°C. When the larvae were placed in 1.5 mL tubes, an approximately 5 mm x 5 mm window was made in the lid of each tube and a 59 μm nylon mesh filter was inserted between the lid and tube. To prevent drying, these 1.5 mL tubes were put in 100-well plastic microtube racks with water-moistened papers. To quantify pupariation rate and developmental time, the number of pupae in each tube/vial was counted and recorded for at least 20 days. On rare occasions, almost all of the first instar larvae in a tube or a vial died due to suffocation by clogging of the mesh filter with the moist food source, or to their escape from dried food. We did not score such tubes or vials. Statistical analyses including a non-parametric two-tailed Mann-Whitney *U* test (for comparison of two samples), a Steel-Dwass test (for comparison of multiple samples) or Steel test (for non-parametric multiple comparisons to a control) were performed. For Figures 3E and 3F, a Steel test was used for comparison of pupariation rates on the M diet with those on the other dietary conditions in each species or genotype. Each point in Figures 1D, 3A, 3B, 3E, 3F, 7A–7D, S1D, S1E, S3D, and S5A indicates the percentage of pupated animals out of 20 first-instar larvae in a 1.5 mL tube (Figures 1D, 3A, 3B, 3E, 3F, 7A–7D, S1D, S1E, and S3D) or the percentage of pupated animals out of 200 first-instar larvae in a vial (Figure S5A) with each respective diet. In these figures, *n* represents the number of the 1.5 mL tube or the vial for each condition (the number of the replicate). Each point in Figure S1A indicates averaged developmental time of pupated animals in each 1.5 mL tube, which were prepared for Figure 1D. Tubes with no pupae were omitted to calculate the average time.

Designs for interspecies and omics analyses

Drosophila species can vary in many ways, including the amount of food consumed (Figures S1B and S1C), and these interspecies differences should be considered in setting up studies and designing experiments (Markow and O'Grady, 2005). We therefore compared phenotypes among the three diets within each species, rather than between the species on the same diet.

As for omics analyses, considering two issues in the sample preparations, as described below, we compared larvae that could develop to the wandering larval stage on the M diet with those on the P diet. The first issue was matching the developmental stage and sex. The entire developmental time to pupariation was different between the species and between the diets (Figure S1A), implying that the time at each instar may also be variable. Those differences can profoundly influence the outcome of the experiments and lead to erroneous conclusions (Markow and O'Grady, 2005). In order to avoid such misleading conclusions, it is necessary to compare larvae at the same developmental stage. It is also critical to exclude sex-related differences in profiles of gene expression and metabolites, because development of gonads has already begun during larval stages (Cooper, 1950). With these conditions in mind, we opted to select male larvae at the wandering third-instar stage that fed on the M or the P diet, especially for reasons concerning *D. sechellia*, as follows: sexing live larvae of each species depends on finding the testes, but testes of *D. sechellia* are much smaller than those of the other four species; consequently, it is sometimes very hard to discriminate *D. sechellia* males from females, even at the wandering larval stage. As long as we positively select males, no error arises. Hence, we considered that choosing males at the wandering larval stage ensured the reliability of the experiments. The second issue is collecting sufficient sample amounts. The major limiting factor for our omics experiments is the sample preparations of *D. sechellia* larvae. Collecting first-instar *D. sechellia* larvae is far more labor-intensive than collecting those of *D. melanogaster*, chiefly because *D. sechellia* females have an inherent low egg laying potential due to a low ovariole number and low egg production (R'Kha et al., 1991, 1997). To perform omics experiments using wandering third-instar larvae, we needed approximately seven times more adult flies for egg collection of *D. sechellia* than *D. melanogaster.* In addition, we picked up newly hatched first instar larvae one by one, placed them on each diet, and collected them at the wandering larval stage. Scaling up for *D. sechellia* in our experiments, particularly in GC-MS, was exceedingly difficult to perform.

The outcomes of our comparisons of the M diet-reared wandering third-instar larvae with the P-reared larvae were compelling with respect to distinct patterns of gene expression (Figures 4B and 5B) and amounts of metabolites (Figures 6A–6C). Moreover, differences in metabolic gene expression and metabolites between the wild-type *D. melanogaster* and the *daw* mutant were significantly greater on the M diet than on the P diet (Figures S5B and S5C). These results indicate that our omics experiments using wandering third-instar larvae on the M or the P diet successfully detect detrimental effects of dietary carbohydrate on larval growth of *D. sechellia*, *D. elegans*, and *D. melanogaster daw* mutants.

As mentioned above, we mainly compared phenotypes between the diets within each species. In Figures 5B and 5D, we compared the expression values of the metabolic Daw-repressed genes between the species and found that many of the expression values of those genes were markedly higher in *D. sechellia* compared to the *daw* mutant. From this result, we discussed the possibility that *D. sechellia* may have additional defects in other regulatory mechanisms distinct from TGF-β/Activin signaling (Figure 7E). However, this comparison between the species comes with a caveat, as the amounts of food consumed by *D. sechellia* were less, in general, than the amounts consumed by *D. melanogaster* on all three diets (Figures S1B and S1C), which raises a concern that we compared well-fed *D. melanogaster* with semi-starved *D. sechellia*. Because responses of *D. sechellia* to (semi-)starvation have not been reported, we cannot rule out this alternative possibility.

Scoring of developmental progression

Newly hatched first instar larvae were collected and placed in 1.5 mL tubes containing the individual diets as described above (4 or 5 tubes were prepared per experimental condition). After 95–98 hours or 11 days (see Results), we counted the number of live or dead animals found in each tube and staged individual larvae by tracheal morphology as previously described (Niwa et al., 2010). Color bars in Figures 1E, 1F, 3C, and 3D indicate percentages of live first-instar larvae (blue), live second-instar larvae (green), live third-instar larvae (yellow), pupae (orange), adults (pink), dead first-instar larvae (light gray), dead second-instar larvae (dark gray), and dead third-instar larvae (brown). Percentages of animals that could not be found (Not found) are shown in white. *n* in these figures represents the number of animals for each condition. Images of animals at 98 hr on each diet were acquired with a digital camera (Olympus, DP21) attached to a stereo microscope (Olympus, SZX7).

Feeding assays

20 first instar larvae were transferred to each respective diet containing 1% (w/v) Brilliant Blue FCF (WAKO, #027-12842) for 3 hr. Larvae were washed in PBS and mounted in 50% glycerol. Images were acquired on a Nikon ECLIPSE E800 microscope (Nikon) using Axiovision v3.1 acquisition software (Carl Zeiss). We manually extracted blue pixels from the original images by using Adobe Photoshop, converted them to 8-bit format, and measured the sum of the pixel values (''RawIntDen'') by using Fiji (ImageJ). Statistical analysis was performed using a Steel-Dwass test. *n* represents the number of animals for each condition.

Microbe-swapping experiments

The C, M, and P diet were cooked as described above and dispensed into 50 mL tubes. Microbes associated with *D. melanogaster* or *D. sechellia* were provided by exposing each diet to 20 male flies for 24 hr as described (Piper et al., 2014). After removing the male flies, we mashed these foods and put them into 1.5 mL tubes. Germ-free animals were generated as previously described (Ryu et al., 2008). Embryos (0–18 hr after egg laying) were dechorionated for 3 min in 50% bleach, then washed with sterile water. These dechorionated embryos were subsequently washed in 70% ethanol for 5 min, followed by two washes with sterile water. These germ-free embryos were transferred onto apple agar plates using an autoclaved brush. 20 newly hatched larvae were collected and placed in 1.5 mL tubes with each diet that had been exposed to microbes.

GC-MS analysis of resources in the wild

We collected two species of fermented wild morning glory (*Ipomoea indica* and *Ipomoea cairica*), in May, 2015, in Okinawa, Japan. We dissected fallen flowers of these morning glories, and those on which the second- or the third-instar *D. elegans* larvae had grown were used for analysis. After *D. elegans* larvae were removed, only fermented stamens, pistils, and pollen were transferred to 1.5 mL tubes, frozen on dry ice, sent to the Uemura laboratory, and stored at −80°C. To analyze components of foods that the wild generalists fed on, we placed trap bottles containing fresh Cavendish bananas (*Musa* spp.) or ''Oishi-wase'' plums (*Prunus salicina*) outside our houses in Kyoto for about 1.5 days. We collected flies in the traps and identified the species (Table S1B). In order to match the degree of fermentation between the natural foods, including wild morning glory above, each fruit in the trap bottles was incubated at 25°C for 2 days when larvae grew to the second- or the third-instar stage. After larvae were removed, fermented bananas or plums were transferred to 2 mL Eppendorf tubes, flash frozen in liquid nitrogen, and stored at −80°C. 3 biological replicates of wild morning glory and 3 technical replicates of other samples were prepared and analyzed (each *Ipomoea indica* sample was approximately 80 mg and other samples were approximately 110 mg). Sample processing and targeted GC-MS analysis were performed by Kazusa DNA Research Institute using a SHIMADZU QP-2010 Ultra. In order to narrow down key compounds that characterize the difference of the natural foods, we performed principal component analysis (PCA), which has been widely used for dimensionality reduction of metabolomic data. Before performing PCA, we processed the resulting raw data (peak area normalized by weight and the peak area of an internal standard, Ribitol; Table S1C) by Pareto scaling for (1) minimizing the noise effect, (2) reducing the influence of intense peaks, and (3) avoiding over-manipulating the data (Worley and Powers, 2013; Xi et al., 2014). The raw data were processed using MetaboAnalyst (Xia et al., 2015). Settings for data processing were as follows: Data Filtering ''Interquantile range (IQR),'' Sample normalization ''None,'' Data transformation ''None,'' and Data scaling ''Pareto scaling.'' We processed raw data from 12 samples (4 sample types x 3 replicates) and performed principal component analysis using ggbiplot of R (Figure 2C). To generate the heatmap and plots of compounds with large contributions to PC1 (Figures 2D and 2E), we used the raw data (peak areas normalized by weight and the peak area of an internal standard, Ribitol). Images of native foods in Figure 2B were obtained with a Stylus TG-4 Tough camera (Olympus).

Nutrients in unfermented natural foods

We obtained carbohydrate contents, protein contents, and fat contents of unfermented natural food resources for *D. melanogaster* (fruits and vegetables; described in Broderick and Lemaitre, 2012 and Gibson et al., 1981), *D. sechellia* (*M. citrifolia* fruits), *D. elegans* (*Alpinia* flowers), and *D. erecta* (*Pandanus* fruits) from the USDA Food Composition Databases (fruits and vegetables; US Department of Agriculture Agricultural Research Service Nutrient Data Laboratory, 2018), Malaysian Food Composition Database (*M. citrifolia* fruits; Tee et al., 1997), Rachkeeree et al., 2018 (*Alpinia* flowers) or Dignan et al. (2004) (*Pandanus* fruits). P:C ratios of the individual foods (Figure 2F) were calculated by dividing the values of protein contents by those of carbohydrate contents. The data shown in Figures 2F and S2 were sorted by their P:C ratios.

Sample preparation for RNA-seq

For RNA-seq using wandering third-instar larvae, animals were grown in 1.5 mL tubes containing the M or P diet as described above. To prepare each replicate, Trizol (Invitrogen) was used to extract total RNA from 5 whole bodies, 6 dissected muscle/epidermis, 10 dissected midguts, or 10 dissected fat bodies of male wandering third-instar larvae. For dissection of muscle/epidermis, we everted larvae, then removed attached tissues such as discs and fat bodies. For dissection of midguts, malpighian tubules attached to posterior midguts were removed. For dissection of fat bodies, adjacent tissues such as testes and tracheae were removed. To obtain animals for RNA-seq using first-instar larvae, sexually mature adults were placed on apple agar plates with yeast paste and allowed to oviposit for 3 hr (*D. melanogaster CS* and *D. sechellia*) or 5 hr (*D. melanogaster daw* mutant). Newly hatched larvae (20–28 hr after egg laying) were collected and placed in 1.5 mL tubes containing the C or P diet. After 15 hours, live and visibly feeding first-instar larvae were collected and used for RNA extraction (20 animals per replicate).

Further purification of extracted RNA was carried out with a RNeasy Mini Kit (QIAGEN). The purity of RNA was assessed with a BioAnalyzer (Agilent Technologies). For each experiment, three or four biological replicates were analyzed. RNA-sequencing was performed on either an Illumina HiSeq 2500 or an Illumina NextSeq 500 using single end reads. The complete information of RNA-seq can be found in Table S6C.

Analysis of RNA-sequencing

Obtaining files

FASTA files were downloaded from FlyBase (*D. melanogaster* r6.04, *D. simulans* r2.01, *D. sechellia* r1.3, *D. erecta* r1.04; Clark et al., 2007; Hu et al., 2013) or NCBI (*D. elegans* r2.0; Chen et al., 2014). Transcript annotation files (dmel-all-r6.04.gtf, dsim-all-r2.01.gtf, dsec-all-r1.3.gtf, dere-all-r1.04.gtf; Clark et al., 2007; Hu et al., 2013) and tissue-type specific RNA-seq datasets of *D. melanogaster* (gene_rpkm_report_fb_2015_01.tsv; Brown et al., 2014) were obtained from FlyBase. A transcript annotation file of *D. elegans* was converted from an annotation file of *D. melanogaster* as follows: the file was first converted to Bed format by using gtf2bed (ver. 2.4.12; Neph et al., 2012), then converted to that of *D. elegans* by using a command line liftOver tool of the UCSC Genome Browser and a LiftOver file dm6ToDroEle2.over.chain (https://hgdownload-test.cse.ucsc.edu/goldenPath/dm6/liftOver/) with -minMatch = 0.1 option, and finally converted to a gtf-formatted file using the awk command. Files of orthologous gene symbols (Waterhouse et al., 2011) and NCBI GeneIDs of all genes in the *D. melanogaster* were downloaded from FlyBase using the Batch Download tool. KEGG gene IDs (Kanehisa et al., 2017) were downloaded from KEGG API (http://rest.kegg.jp/conv/dme/ncbi-geneid).

Trimming

All raw sequencing data were adaptor trimmed using TagDust (ver. 1.13; Lassmann et al., 2009) with -fdr 0.05 option. The data were then quality trimmed by using Fastx-toolkit (ver. 0.0.14; http://hannonlab.cshl.edu/fastx_toolkit/): fastx_trimmer (except for data obtained from the ''Genome Science'' program) with -Q 33 -f 14 -l 100 options, fastx_clipper with -a N option, fastq_quality_filter with -q 20 -p 80 options, and fastq_quality_trimmer with -t 20 option.

Mapping and differential expression analysis

To identify differentially expressed genes, we basically followed Anders et al. and Loraine et al. (Anders et al., 2013; Loraine et al., 2015). Trimmed fastq files were mapped using Tophat (ver. 2.0.13; Kim et al., 2013), utilizing Bowtie2 (ver. 2.2.3.0; Langmead and Salzberg, 2012) to each genome while supplying transcript annotation. The BAM files generated by mapping were sorted and converted to SAM files using SAMtools (ver. 1.1; Li et al., 2009). Gene-based read counts were then obtained using htseq-count (ver. 0.6.1p1; Anders et al., 2015) with -s no -a 10 options. Differential expression analysis was performed on the count data using a generalized linear model (GLM) in the edgeR Bioconductor package (ver. 3.10.2; McCarthy et al., 2012; Robinson et al., 2010). Raw p values were adjusted for multiple testing with the Benjamini–Hochberg procedure. Differentially expressed (DE) genes with an adjusted p value lower than 0.05 were considered to be statistically significant. To compare RNA-seq data between the species, the output files from edgeR were combined into one file (Tables S6A and S6B) using custom Perl scripts. Data for each gene of *D. simulans, D. sechellia* or *D. erecta* were added to that of *D. melanogaster* if the gene was a 1:1 ortholog of a *D. melanogaster* gene, to make a combined file. Data for *D. elegans* were directly added to the combined file. This was possible because a transcript annotation file of *D. elegans* had been converted from that of *D. melanogaster*, and consequently, gene names of *D. elegans* were the same as those of *D. melanogaster*. For the heatmaps in Figures 4B, 5B, 5D, S3A, and S4A, heatmap.2 in the gplots package of R was used. A functional annotation clustering of Daw-repressed genes was performed by using the Functional Annotation Clustering of DAVID (Huang et al., 2009). p values were calculated with a modified Fisher's test, and then enrichment scores (the geometric means

of all the enrichment p values of each annotation term in the clusters) were calculated (Figures S4B–S4D; Tables S2N, S3K, and S5I). For gene ranking in Figure 4C, we used adjusted p values and $\log_2$-transformed fold change (Log_2FC) calculated by edgeR, and ranked genes by signed adjusted p values, where the signs were from Log_2FC. Genes with the same adjusted p value were ranked based on Log_2FC. A two-tailed Mann-Whitney *U* test was performed to compare gene ranking in *D. melanogaster CS* "K" with that in *daw* mutants. A Steel test was performed to compare gene ranking in *D. melanogaster CS* "G" with that in *D. simulans* or *D. sechellia*, or to compare gene ranking in *D. melanogaster CS* "N" with that in *D. elegans* or *D. erecta*. We used the KEGG Mapper Search&Color Pathway tool (Kanehisa et al., 2012) for mapping DE genes and metabolites on the *D. melanogaster* metabolic pathways (Figures 5A, 6B, S5B, and S5C). BioVenn (Hulsen et al., 2008) was used to construct a Venn diagram (Figure 5C).

qRT-PCR of germline-less or control larvae

To obtain germline-less male larvae (Figures S3B and S3C), we crossed osk^{301}/osk^{301} females to *Sxl-eGFP* males (J. Thompson et al., 2004, 45th Annual Drosophila Research Conference, conference). Because of the difficulties in finding testes in the germline-less male larvae, we relied on the lack of *Sxl-eGFP* expression (*Sxl-eGFP* is a marker for female embryos) and picked up male embryos (11–16 hr after egg laying); this genetic approach obviated the difficulties in choosing only male larvae by their testes. As a control, male embryos from *Sxl-eGFP* females crossed to *CS* males were picked up. The respective male embryos of each genotype were transferred onto separate apple agar plates, and 20 newly hatched larvae were collected and placed in 1.5 mL tubes with each diet. Trizol (Invitrogen) was used to extract total RNA from 3 whole bodies of male wandering third-instar larvae per replicate. RNA samples were treated with an RNase-Free DNase set (QIAGEN), and further purified using an RNeasy Mini Kit (QIAGEN). 500 ng of total RNA was used as a template for cDNA synthesis using a ReverTra Ace qPCR RT Kit (TOYOBO). qRT-PCR was performed by mixing cDNA samples diluted 10-fold with THUNDERBIRD SYBR qPCR Mix (TOYOBO). *n* represents the number of the biological replicate for each condition. Expression levels were normalized against those of *rp49*. Data were analyzed using the comparative C_T method on a StepOnePlus Real-Time PCR System (Applied Biosystems). A gene was considered not detectable when $C_T > 32$. Statistical analysis was performed using one-way ANOVA with Tukey's post hoc test (for comparison of multiple samples). The following primers were used:

CG31226 forward: 5′- GCTATCCTTGCTATCCTTGCG
CG31226 reverse: 5′- TCCGTTGTAGGGTCCAAAGC
CG31644 forward: 5′- ACACTTTACACAACAATCCGC
CG31644 reverse: 5′- GGAGGACAGGACGATAGGTA
rp49 forward: 5′- CAGTCGGATCGATATGCTAAGCTG
rp49 reverse: 5′- TAACCGATGTTGGGCATCAGATAC

GC-MS analysis of whole larvae

10 male wandering third-instar larvae were collected to prepare one biological replicate, and were washed with PBS to remove all traces of food. Larvae were transferred to 1.5 mL tubes, weighed on a microbalance (Sartorius, CP225D), and then flash frozen in liquid nitrogen. 6 replicates per condition were prepared and analyzed. Sample processing and targeted GC-MS analysis were performed by the Metabolomics Core Research Facility at the University of Utah School of Medicine according to the method described in Tennessen et al. (2014). The resulting raw data (peak areas normalized by weight; Table S7C) were uploaded in MetaboAnalyst, and subsequent data processing and analyses were performed using this tool. Settings for data processing were as follows: Data Filtering "None," Sample normalization "None," Data transformation "None," and Data scaling "Pareto scaling." For statistical comparison of 2 sample types (Figures 6B and 6C; Table S7A), we processed raw data from 12 samples (2 sample types x 6 replicates) and performed Volcano Plot analysis with options "Non-parametric tests" and "FDR-adjusted." Statistically significant changes of metabolite amounts were defined as those with an adjusted p value lower than 0.05. To generate the heatmap of metabolite amounts (Figure 6A), we processed raw data from 24 samples (4 sample types x 6 replicates), scaled the processed data by Z scaling (genescale function of R), and made a heatmap (heatmap.2 of R).

Lipid droplets in fat bodies

Male wandering third-instar larvae were dissected in PBS, and fixed with 10% formalin in PBS for 20 min. The fixed tissues were washed with PBS, incubated in 1 μg/ml Nile Red (Sigma-Aldrich) diluted in PBS for 30 min, washed with PBS, and mounted in VECTASHIELD Mounting Medium with DAPI (Vector Laboratories). Slides were imaged within 30 minutes to 1.5 hours after mounting, using a Nikon C1 laser scanning confocal microscope coupled to a Nikon Eclipse E-800 microscope. Along the anterior-posterior axis, middle regions of the fat bodies were imaged using the 60x Oil objective with an electronic zoom of 2, 1 μm interval, and a resolution of 512 × 512. Under each genotype and dietary condition, fat bodies of five larvae were imaged for quantification of lipid droplet size. Among optical sections of each microscopic field, the section was selected where the size of DAPI-stained nuclei was the largest. We first used Photoshop to perform levels adjustment and mask areas with weak signals. We then conducted smoothing, binarization, watershed segmentation, and quantification (Analyze Particles) using NIH ImageJ software. To focus on large lipid droplets, we compared distributions of droplet size over 2000 pixels (86.09 μm^2). Statistical analysis was performed using a Steel test to compare lipid droplet area of *D. melanogaster CS* on the P diet with that of each sample.

QUANTIFICATION AND STATISTICAL ANALYSIS

All statistical analyses were performed using R (R Core Team, 2017). Values of $p < 0.05$ were considered statistically different. The experiments were not randomized or blinded. No statistical method was used to determine whether the data met assumptions of the statistical approach. For statistical analyses of RNA-seq and GC-MS data, see Tables S2, S3, S4, S5, S6, and S7A–S7C, and each section of STAR Methods. As for other experiments, statistical tests used, the exact sample size (*n*), and p values are shown in Table S7D. See also STAR Methods and figure legends for details.

DATA AND CODE AVAILABILITY

All the RNA-sequencing data have been deposited and are available in the DDBJ Sequence Read Archive. The accession numbers for the data are DDBJ: DRA004295, DRA006831, and DRA007810 (BioProject accession number: PRJDB4481). GC-MS datasets are available within the Supplemental Information.